Two-dimensional van der Waals materials and their mixed low-dimensional hybrids for electrochemical energy applications

Chu Te Chen, Yu Fu, Xin Gao, Anthony Butler, Kristofer Reyes, Huamin Li, Michael Pentaris, Ajay Yadav, Keith T. Wong,* Hongyan Yue,* and Fei Yao*

Compared with their three-dimensional counterparts, two-dimensional (2D) van der Waals (vdW) materials exhibit quantum confinement where charge carriers are spatially confined at the physical boundaries. Particularly, when mixing 2D materials with other low-dimensional (LD) materials, they exhibit enormous potential in electrochemical energy applications due to the reduced dimensionality and, more importantly, material integration synergy, resulting in controllability over mixture composition, layer stacking and arrangement, and interlayer coupling. In this article, the latest advancements in 2D vdW heterostructure and their mixed low-dimensional hybrids (MLDHs) are reviewed with an emphasis on innovations covering hybrid structure construction and electrochemical applications. Recent developments leveraging the 2D vdW platform to promote a mechanistic understanding of charge-transport dynamics at the electrified interface were highlighted. Fundamental insight into the synergistic effect of MLDH integration for advancing the development of electrochemical energy applications was discussed. The knowledge gained on how mixed-dimensional physics and chemistry influence the performance of metal ion batteries and electrocatalytic hydrogen evolution reaction will shed light on the design principle of the electrode materials and deepen the understanding of the process–structural–property–performance relationship of the vdW-based MLDHs.

Introduction

The growing global energy demands along with concerns about materials scarcity and environmental impact have intensified the need for exploring new materials for energy technology development. Two-dimensional (2D) van der Waals (vdW) layered materials, a class of materials composed of atomically thin layers held together by weak vdW interactions, have emerged as highly promising candidates for driving innovation in electrochemical energy applications owing to their rich material chemistry, versatile structure engineering possibility, and tunable surface chemistries.[1–4] Since the rise of graphene, various 2D vdW materials such as transition-metal dichalcogenides (TMDs),[1,5–10] black phosphorus (BP),[11] hexagonal boron nitride (*h*-BN),[5,12] and transition-metal carbides/nitrides/carbonitrides (i.e., MXenes)[13] have been discovered. Unique properties and phenomena have been explored in 2D vdW with decreased layer numbers such as enhanced quantum confinement, active edge site effects, and structural phase transformation,[14–18] enabling a deeper understanding of the fundamental physics and practical applications of 2D vdW layered materials.

Despite extensive research efforts in advancing the electrochemical performance of 2D vdW materials, inherent

Chu Te Chen, Department of Materials Design and Innovation, University at Buffalo, The State University of New York, Buffalo, USA; chuteche@buffalo.edu
Yu Fu, Department of Materials Design and Innovation, University at Buffalo, The State University of New York, Buffalo, USA; yfu5@buffalo.edu
Xin Gao, School of Materials Science and Engineering, Harbin University of Science and Technology, Harbin, China; gaoxin6825@126.com
Anthony Butler, Department of Materials Design and Innovation, University at Buffalo, The State University of New York, Buffalo, USA; afbutler@buffalo.edu
Kristofer Reyes, Department of Materials Design and Innovation, University at Buffalo, The State University of New York, Buffalo, USA; kreyes3@buffalo.edu
Huamin Li, Department of Electrical Engineering, University at Buffalo, The State University of New York, Buffalo, USA; huaminli@buffalo.edu
Michael Pentaris, Custom Electronics, Inc., Oneonta, USA; mpentaris@customelec.com
Ajay Yadav, Applied Materials, Inc., Santa Clara, USA; ajay_yadav@amat.com
Keith T. Wong, Applied Materials, Inc., Santa Clara, USA; keith_wong@amat.com
Hongyan Yue, School of Materials Science and Engineering, Harbin University of Science and Technology, Harbin, China; hyyue@hrbust.edu.cn
Fei Yao, Department of Materials Design and Innovation, University at Buffalo, The State University of New York, Buffalo, USA; feiyao@buffalo.edu
*Corresponding author
Chu Te Chen and Yu Fu have contributed equally to this work.
doi:10.1557/s43577-023-00597-2

material property challenges need to be addressed when employed as MIBs electrodes and HER catalysts. First, 2D layers tend to reassemble or restack during synthesis, especially in solvent processes, due to the existence of vdW interactions and the tendency of surface energy minimization, leading to reduced interlayer distance and limited use of surface area and active sites.[19] Second, despite the well-acknowledged presence of active edge sites, strategies to activate the inert basal planes and increase the total number of active sites in 2D vdW layers need to be introduced. Third, many 2D materials such as the TMD family exhibit low electrical conductivity, especially along the out-of-plane direction, which hinders efficient electron transport, and therefore, overall reaction kinetics.[20] Finally, 2D vdW materials could suffer from property degradation via structural changes, oxidation, or dissolution under harsh electrochemical conditions, adversely affecting the long-term stability of electrochemical devices.[21]

Fortunately, hybrid structures can be created by combining different 2D vdW layers or integrating them with zero-/one-dimensional (0D/1D) materials. These mixed low-dimensional hybrids (MLDHs) not only harness the unique properties of each component, but also overcome the limitations of individual low-dimensional (LD) materials. Mixing materials with different dimensionalities offers the ability to tailor and engineer the properties of 2D vdW layers by precisely controlling their composition, layer stacking and arrangement, and interlayer coupling, resulting in structural synergy for improved electrochemical performance. Furthermore, the investigation of MLDHs will also deepen our fundamental understanding of 2D-vdW-based physics. For instance, creating Moiré superlattice (MS) in twist-angle 2D vdW layers has resulted in boosted electrochemical catalytic activity, opening up avenues for designing vdW materials for improved device performance.

In this article, representative integration techniques for building 2D/2D vdW heterostructures and their mixed dimensional 1D/2D, 0D/2D hybrids will be introduced. Electrochemical energy applications of the previously mentioned nanocomposites used as electrode materials in MIBs and as electrocatalysts for hydrogen evolution reaction (HER) will be reviewed. Recent developments leveraging the 2D vdW layers in conjunction with a microreactor platform to promote a mechanistic understanding of charge-transport dynamics at the electrified interface will be discussed. In the end, discussions on challenges and future perspectives will be provided.

Integration techniques of 2D vdW heterostructures and their MLDHs

Material property optimization through rational structural design requires a diverse range of dimensional mixing. Integration techniques of mixed dimensional hybrids with control over composition, morphology, and structure are essential. Various synthetic strategies, including solid-state reaction,[22–24] electrospinning,[25–27] chemical vapor deposition (CVD),[28–32] sol–gel method,[33,34] self-assembly,[35,36] and hydrothermal/solvothermal techniques[32,37,38] have been widely employed for constructing hybrid nanocomposites. Extensive literature reviews have documented the success of the LD mixing techniques, and interested readers are referred to References 22, 32, 37, 39–41. In this section, we aim to highlight the representative synthesis methods and review the recent innovative examples in the preparation of vdW heterostructures and their MLDHs.

Single-step techniques

Chemical vapor deposition

In the chemical vapor deposition (CVD) process, precursors decompose or react with the substrate at a specific temperature within a hot-environment chamber. This technique has the potential to precisely control the growth of materials at the nanoscale and it has been widely used to prepare LD materials such as 1D carbon nanotubes (CNTs),[42–44] 2D layered graphene,[45–48] TMDs,[49–51] and MXenes.[13,52–54] Lately, significant research progress has been made in constructing vdW heterostructures and their MLDHs using CVD.

2D/2D vdW heterojunctions

CVD has been employed as a powerful tool to assemble ultrathin 2D/2D vdW heterostructures. Strategies to engineer the interlayer coupling by controlling the stacking sequence and stacking arrangement (vertical or in-plane) of TMD/TMD heterobilayers during the CVD process have been developed and widely reviewed.[22,40,41,49,51,55] It is worth mentioning that vertical stacked 2D/2D homojunctions (such as graphene/graphene and TMD/TMD) with small twist angles have been achieved recently using CVD as well,[51,56] providing new opportunities to tune the interlayer electronic coupling and thus influencing charge-transfer kinetics in the electrochemical process (more discussion can be found in the section "Mechanics understanding of electrochemical processes based on vdW-based MLDHs").[57–60] Benefiting from the recent advancements in CVD MXene growth, 2D/2D graphene/MXene and TMD/MXene heterostructures have also been produced.[29,30,61,62] For instance, Xu et al. successfully demonstrated direct CVD growth of high-quality graphene/α-Mo_2C vertical heterostructures with uniformly well-aligned lattice orientation and strong interface coupling. In the heterostructure, both graphene and α-Mo_2C crystal showed no defect, and the graphene is strongly compressed.[31] Jeon et al. conducted a study on the chemical conversion of MoS_2 to Mo_2C to form a lateral junction with thermal annealing, as shown in **Figure 1**a. The result revealed that the thermal annealing duration can be adjusted to achieve a partially converted semiconducting material or a fully converted metallic Mo_2C. The resultant Mo_2C/MoS_2 hybrid junction exhibits a metallic/semiconducting junction nature with an atomically sharp interface (Figure 1b) and low contact resistance.[30]

Two-dimensional vdW-based MLDHs

Numerous 2D vdW-based MLDHs have been successfully achieved using CVD. In the case of all-carbon-based architecture, parallel and vertical 1D/2D CNT/graphene integrated structures where nanotubes are sandwiched between graphene layers in the forms of randomly aligned networks or vertical pillars, respectively, have been realized using CVD.[63–65] Especially, in the vertical CNT/graphene architecture, seamless contact between the 1D and 2D graphitic layers has been achieved and the poor out-of-plane electron transport originating from the weak vdW interaction in the transverse direction can be improved, resulting in largely reduced contact resistance along with high surface area and meso-/microporosity.[66] Recently, Xiao et al. synthesized a hierarchical 1D/2D carbonaceous structure consisting of CNTs and graphene by employing Fe nanoparticles confined to the interlamination of graphite as a catalyst and porous nickel foam as a scaffold substrate in the in situ template-directed CVD process, as shown in Figure 1c. The obtained structure exhibited a fully 3D interconnected CNT web through the pores of graphene foam (GCNT web) (Figure 1d) with completely geometric, mechanical, and electrical interconnectivity.[67]

In the case of beyond-carbon 2D vdW-based MLDHs, 1D/2D and 0D/2D architectures, especially those that contain carbon species, have been reported using the CVD synthesis technique.[37,67–69] For instance, Li et al. synthesized 1D/2D CNT/TMD hybrids on CNT-coated dielectric substrates in a low-pressure CVD system, as shown in Figure 1e. In this structure, nanotubes serve as favorable heterogeneous nucleation sites for TMDs. Taking MoS_2 as an example, the MoS_2 grains grow on the substrate while bridging the subnanometer gaps beneath the CNTs, as displayed in Figure 1f and g, resulting in the creation of a continuous MoS_2/CNT hybrid film with high conductivity and mechanical stability.[69] Li et al. reported a 1D/2D CNT/MXene structure synthesized by *in situ* grown CNT on delaminated $Ti_3C_2T_x$ nanosheets. The resulting MXene nanosheets were found to be covered and interconnected by the densely packed CNT network.[70] As for the 0D/2D hybrids, we noticed that CVD was not used as often as other solution-based methods such as hydrothermal/solvothermal, sonochemical

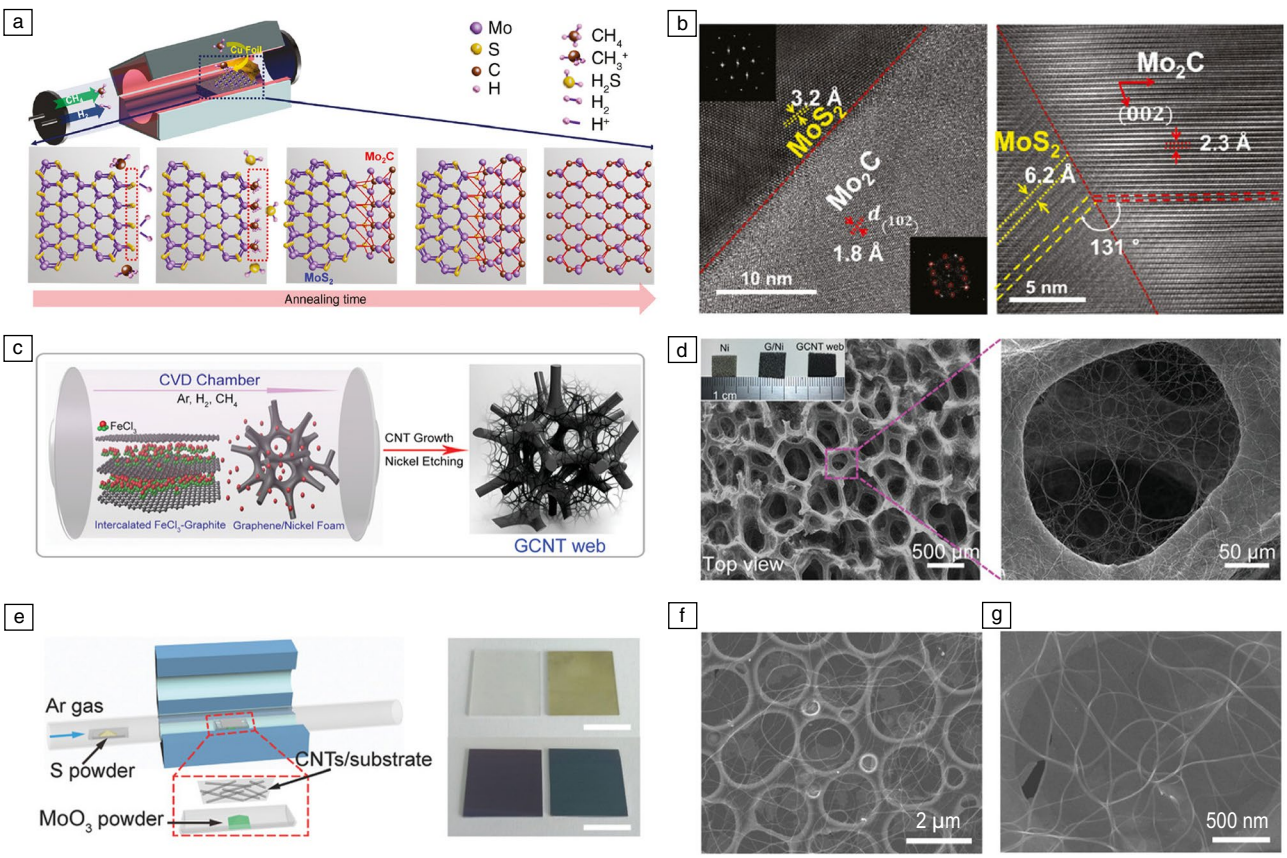

Figure 1. (a) Schematic illustration of chemical vapor deposition (CVD) setup for the synthesis of 2D Mo_2C and 2D/2D Mo_2C/MoS_2 lateral heterostructure. (b) Top and cross-sectional view high-resolution transmission electron microscopy images of Mo_2C/MoS_2 lateral heterostructure. Reprinted with permission from Reference 30. © 2018 American Chemical Society. (c) Schematic illustration of *in situ* growth of 1D/3D carbon nanotube (CNT)/graphene foam (GF) scaffold. (d) Scanning electron microscopy (SEM) images of the graphene carbon nanotube (GCNT) web. Reprinted with permission from Reference 67. © 2018 Wiley. (e) Schematic illustration of CVD setup for 1D/2D CNT/MoS_2 hybrid films and corresponding optical images of different CNT-coated substrates after MoS_2 hybridization. Scale bars, 1 cm; SEM (f) and magnified SEM (g) images of the 1D/2D CNT/MoS_2 hybrid film supported on a copper grid. Scale bars, 2 μm in (f) and 500 nm in (g). Reprinted with permission from Reference 69. © 2018 Wiley.

reaction, or chemical oxidation/exfoliation methods.[71–74] However, it has the potential to produce quantum dots (QDs) in a large area with better controllability.[75–78] For instance, Ding reported the direct synthesis of graphene QDs on insulating hexagonal BN (*h*-BN) substrate by atmospheric pressure CVD without any metal catalyzer. The thickness of the graphene QDs can be controlled by tuning the gas mixing ratio. The *h*-BN substrate induces the formation of high-quality and high-surface-density dots with an ordered arrangement over a large area.[79]

Self-assembly

Self-assembly (SA) organizes material building blocks with different dimensionalities into complex superstructures through noncovalent interactions, such as hydrogen bonding, vdW interactions, electrostatic attraction, hydrophobic–hydrophilic interactions, and π–π interactions.[36,80] Two-dimensional vdW structures, especially chemically modified carbonaceous materials (such as graphene oxide, reduced graphene oxide, etc.) and MXenes are enriched with multiple functional groups, endowing them as desirable materials to assemble with themselves or to form hybrid structures.[36,81–83]

Two-dimensional/2D vdW heterojunctions

The SA method has the universal applicability to create a range of 2D/2D vdW heterostructures and can be effectively extended to produce 2D/2D hybrids in lateral and vertical arrangement fashions.[84–87] For instance, to construct nitrogen-doped graphene (NDG)/MoS_2 heterostructure, dopamine (DOPA) monomers were attached to Li-intercalated MoS_2 layers via an electrostatic-attraction-assisted SA process, followed by in situ conversion of DOPA to NDG. The heterojunctions showed high conductivity, rich active sites, and expanded interlayer spacing. Yun et al. reported 2D/2D MoS_2/WS_2 and $MoS_2/NbSe_2$ heterostructures via fast interfacial SA of chemically exfoliated TMDs from dilute dispersions simultaneously or sequentially, leading to the formation of lateral and vertical vdW heterostructures, respectively.[87]

One challenge in assembling a 2D/2D heterostructure by SA is how to create electron conductive bridges across nanosheets with regular pore distribution. Recently, Wang et al. intercalated amphiphilic triblock copolymer F127 (PEO-PPO-PEO) and resols into $Ti_3C_2T_x$ MXene where F127 unimers self-assembled into micelles with hydrophobic PPO block and hydrophilic PEO block (with -OH terminal groups) as the cores and shells, respectively, and interacted with the resol molecules through hydrogen bonding. The resulting $Ti_3C_2T_x$-micelle@resol composites were then thermally treated, followed by metal etching and chlorination procedures, leading to the formation of all-carbon-based MLDHs composed of ordered mesoporous carbon (OMC) with MXene-derived-carbon (MDC) nanosheets.[88] Allah et al. reported a $Ti_3C_2T_x$ MXene/nitrogen-doped ordered mesoporous carbon (NOMC) heterostructure (**Figure 2**a) through SA of melamine resol-P123 micelles with exfoliated $Ti_3C_2T_x$ nanosheets. The NOMC is well aligned with the $Ti_3C_2T_x$ nanosheet (Figure 2b–c) and advantageous for preventing MXene sheets from restacking with ordered porous structure.[89]

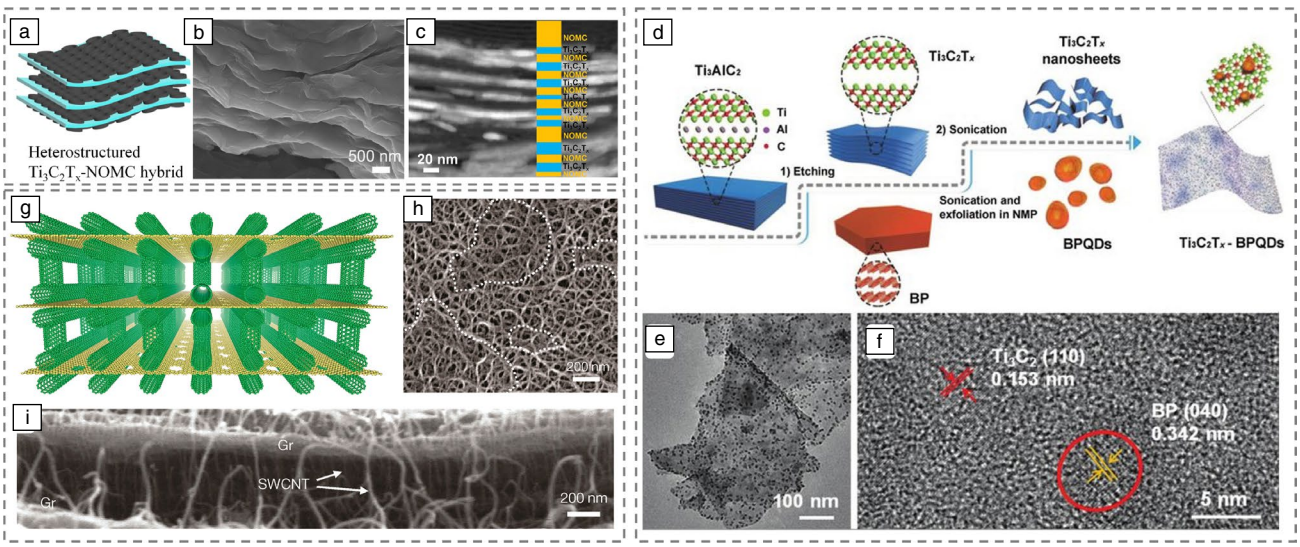

Figure 2. (a) Schematic illustration of the 2D/2D $Ti_3C_2T_x$/nitrogen-doped ordered mesoporous carbon (NOMC) hybrid material. (b, c) Cross-sectional scanning transmission electron microscopy images of $Ti_3C_2T_x$/NOMC hybrid material. Reprinted with permission from Reference 89. © 2019 Elsevier. (d) Schematic illustration of the formation process of the 0D/2D black phosphorus quantum dot (BPQD)/TNS composite. (e) TEM image of the BPQD/Ti_3C_2 nanosheet (TNS) composite. (f) High-resolution transmission electron microscopy image revealing BPQDs anchored on the surface of TNS. Reprinted with permission from Reference 96. © 2018 Wiley. (g) Schematic of the 3D single-walled carbon nanotube (SWCNT)-bridged graphene block. (h) Scanning electron microscopy (SEM) image showing the porous SWCNT network and graphene flakes (dotted lines). (i) Magnified cross-sectional SEM image of the hybrid structure that clearly shows vertical SWCNTs between the graphene layers in the inner part. Reprinted with permission from Reference 97. © 2015 American Chemical Society.

Two-dimensional vdW-based MLDHs

Zero-dimensional (nanoparticles/nanospheres) as well as 1D nanotubes have been successfully integrated with 2D layered structures using SA.[90–95] For instance, Meng et al. reported a synthesis of 0D/2D nanocomposites consisting of black phosphorus quantum dots (BPQDs) and Ti_3C_2 MXene nanosheets (TNSs). The BPQDs and well-dispersed TNSs were first prepared separately, followed by an interfacial assembly of BPQDs on TNSs (Figure 2d). The BPQDs with a size of 0.34 nm were anchored on the nanosheets, as shown in Figure 2e–f. The author found strong covalent interactions (P–O–Ti bonds) at interfaces between BPQDs and TNSs, which enhanced the pseudocapacitive charge storage.[96] Pham et al. assembled a 1D/2D CNT/graphene porous structure based on Coulombic interaction achieved by grafting positively charged CNTs with cationic surfactants onto negatively charged graphene oxide sheets, as shown in Figure 2g. In the structure, vertically aligned CNTs were observed in addition to planar CNT network. Benefiting from the CNT pillared structure with rich porosity induced by KOH activation (Figure 2h–i), the freestanding, flexible, 3D hierarchical structure showed high electrical conductivity and significantly improved accessible surface area, facilitating fast electron and ion transport.[97]

Multistep synthesis

Compared with the single-step method, the multistep synthesis method integrates different synthesis techniques such as electrospinning,[25–27] CVD,[28–32] sol–gel method,[33,34] self-assembly,[35,36] microwave-assisted method,[73,98] and hydrothermal/solvothermal techniques[32,37,38] to produce MLDHs. The multistep synthesis allows for more complex reactions to produce multicomponent hybrids with a high order of structural complexity. As such, MLDHs can be produced with rich chemistry combinations, versatile morphologies, numerous charge-transport channels, and abundant active sites, beneficial for electrochemical applications. In addition, each step can be optimized individually, allowing for fine-tuning the properties of each component and improving overall structural synergy. Numerous MLDHs have been produced using the multistep methods and we recommend a few review papers for interested readers.[22,39,91,92,99] A few recent examples of novel MLDH structures constructed by multistep methods are highlighted next.

He et al. synthesized a freestanding 3D hierarchical structure consisting of few-layered graphene nanosheets sandwiched by 1 T MoS_2 nanosheets by integrating a one-pot hydrothermal process with a freeze-dry method. In addition to the facile electron transfer originating from the high electronic conductivities of graphene and metallic 1 T-phase MoS_2, the porous 3D structure can also advance the ion transfer due to the hydrophilic nature of MoS_2.[38] Chen et al. produced porous hierarchical MoS_2 tubular structures aligned with CNTs using combined electrospinning and hydrothermal processes. Their approach introduces carboxylic groups onto multiwalled CNTs to improve the dispersion of CNT on polyacrylonitrile (PAN) nanofibers during electrospinning (**Figure 3**a). Ultrathin MoS_2 nanosheets were then integrated into the CNT/PAN hybrid structure using the hydrothermal method, followed by porosity creation at the expense of Co nanoparticles. A schematic illustration of the unique CNT-wired porous hierarchical MoS_2 nanotubes is shown in Figure 3b.[26] Cui et al. synthesized a 1D/2D hybrid material by integrating MoS_2 and carbon fiber (CF), namely (MoS_2/CF)@MoS_2@C (Figure 3c–h), via combined electrospinning, hydrothermal, and postannealing approach. The resultant multicomponent MLDH exhibited remarkable sodium storage capacity, which can be attributed to its highly conductive, cross-linked 3D framework as well as the protective function of the outermost carbon layer.[27] Ren et al. reported a method for creating a 0D/2D/2D hybrid foam composed of CNTs, graphene, and MoS_2 nanoparticles. The graphene foam (GF) was produced on nickel foam using the CVD method. CNT was then dispersed in alcohol and applied to the GF, creating GF@CNT. Ammonium thiomolybdate powders were added to the GF@CNT hybrid followed by a hydrothermal process, resulting in ternary GF@CNT@MoS_2 MLDHs.[100]

Two-dimensional vdW heterostructures and their MLDHs for electrochemical energy applications

LD materials have emerged as promising candidates for electrochemical energy applications. These materials exhibit unique physicochemical properties due to the quantum confinement effect arising from the reduced dimensionality. Furthermore, enhanced properties and expanded applications can be expected by forming MLDHs via material hybridization or composite design, allowing for the optimization of various material characteristics for specific applications.[93,99,101–106] In the following section, we will highlight the recent achievement of MLDHs in the application of MIBs and HER.

Two-dimensional/2D vdW heterostructures

Two-dimensional/2D heterostructures such as MoS_2/carbon nanosheets,[107] MoS_2/graphene,[108–119] $MoSe_2$/graphene,[120–126] WS_2/graphene,[127,128] $Ti_3C_2T_x$/graphene,[129–133] MoS_2/$Ti_3C_2T_x$,[134–140] MoS_2/Mo_2CT_x,[141] $MoSe_2$/$Ti_3C_2T_x$,[134,142,143] have been investigated in electrochemical applications. The 2D hybrids exhibit structural synergy in terms of enlarged surface area, increased electrical conductivity, enhanced structural integrity, and restacking/oxidation prevention, resulting in improved electrochemical performance along with desired structural stability and mechanical flexibility.

As an example, Yuan et al. synthesized a 2D/2D BN/$Ti_3C_2T_x$ hybrid through a solvent-free ball-milling method. Leveraging from the enlarged interlayer spacing, reduced nanosheet size, and better structural integrity, the hybrid structure delivered a capacity of 345 mA h g^{-1} at 1 A g^{-1} with long-cycle stability as a Na-ion battery (SIB) anode.[144] Zhou et al. constructed a super light and bendable MXene/graphene aerogel (MGA) as the Zn host in Zn-ion batteries (ZIBs) via hydrothermal method. Due to the solid zincophilic traits and the presence of micropores within MGA, densely encapsulated

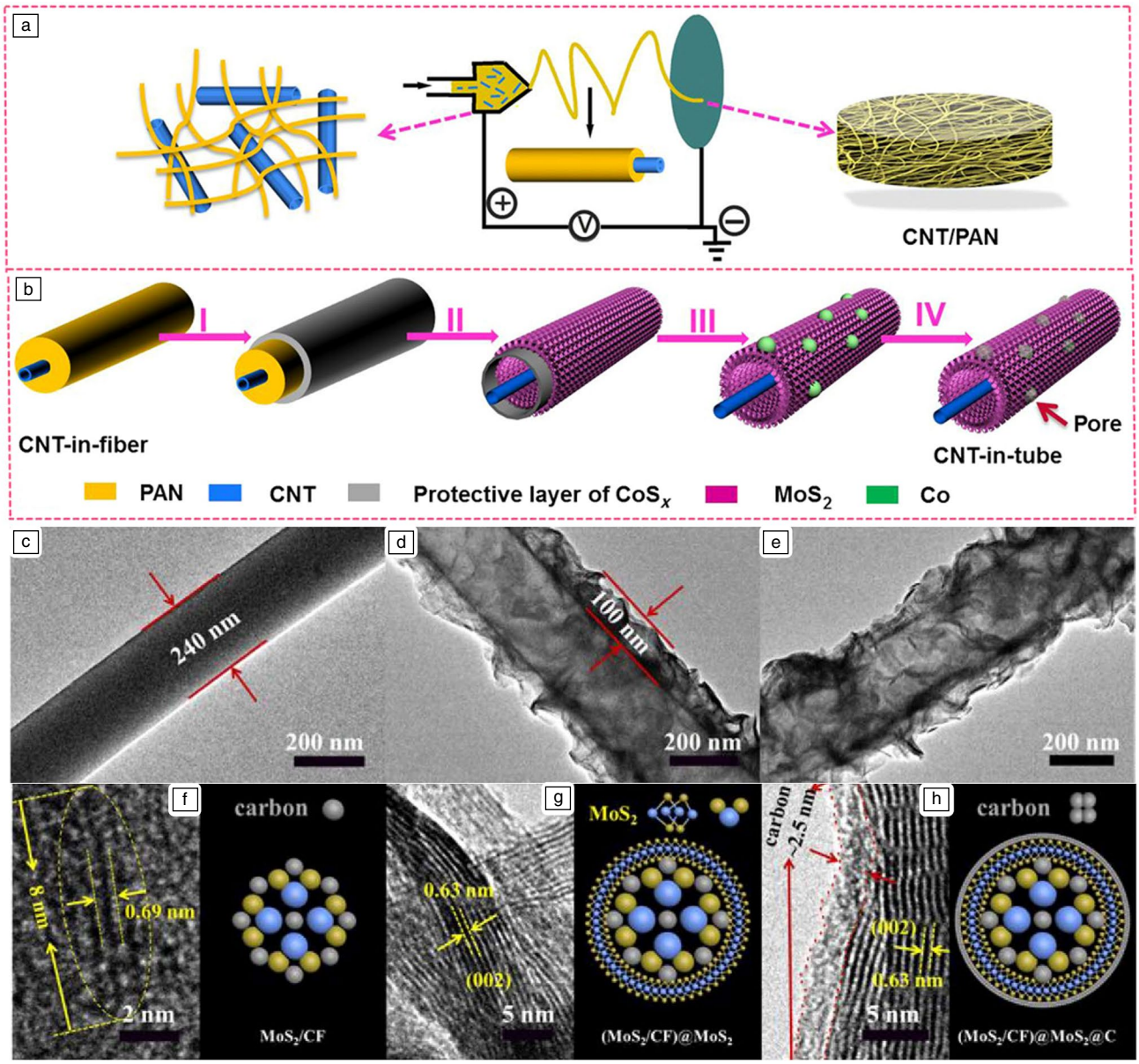

Figure 3. (a) Illustration of the synthesis process of the carbon nanotube (CNT)/PAN tube-in-fiber structure by electrospinning. (b) Schematic of the fabrication process for the CNT-in-tube structure. (I) Growth of a protective layer of CoS_x on the CNT-in-fiber composite. (II) Formation of MoS_2 nanosheets on the composite accompanied by the removal of PAN, yielding a tubular structure. (III) Heating treatment of the hybrid to reduce the CoS_x to Co nanoparticles. (IV) Acid treatment to remove Co particles to obtain a CNT/MoS_2 tubular structure. Reprinted with permission from Reference 26. © 2016 The Authors. Transmission electron microscopy images of (c) 2D/1D MoS_2/CF, (d) (MoS_2/CF)@MoS_2, and (e) (MoS_2/CF)@MoS_2@C. High-resolution TEM images and schematic representation of (f) MoS_2/CF, (g) (MoS_2/CF)@MoS_2, and (h) (MoS_2/CF)@MoS_2@C. Reprinted with permission from Reference 27. © 2018 Elsevier.

Zn can be electrodeposited inside the host structure (**Figure 4**b[i–ii]). Moreover, the MGA maintained a flat top surface without visible pores after Zn deposition, leading to a substantial reduction in the contact area with the electrolyte and thus the suppression of side reactions (Figure 4a). Moreover, this 2D/2D hybrid induces the *in situ* formation of the solid electrolyte interface (SEI) containing zinc fluoride due to the presence of inherent –F terminations on MXene. The zinc fluoride-based SEI effectively inhibits the growth of dendritic structures, enhancing the stability and safety of the battery. Consequently, the MGA@Zn anode demonstrated a stable cycling profile for more than 1000 h at a current density of 10 mA cm^{-2} with a fixed capacity of 1 mAh cm^{-2} (Figure 4b). In addition, a smoother and dendrite-free surface was observed when compared with the Cu@Zn anode (Figure 4b[iii–iv]).[131]

As demonstrated by Fan et al., 2D/2D MoS_2/graphene nanohybrids can be employed as a cathode in hybrid-ion (Mg^{2+}/Li^+) batteries. In their process, MoS_2 nanosheets were synthesized on CVD-grown graphene via the hydrothermal method. Due to the highly conductive nature of graphene and the expanded

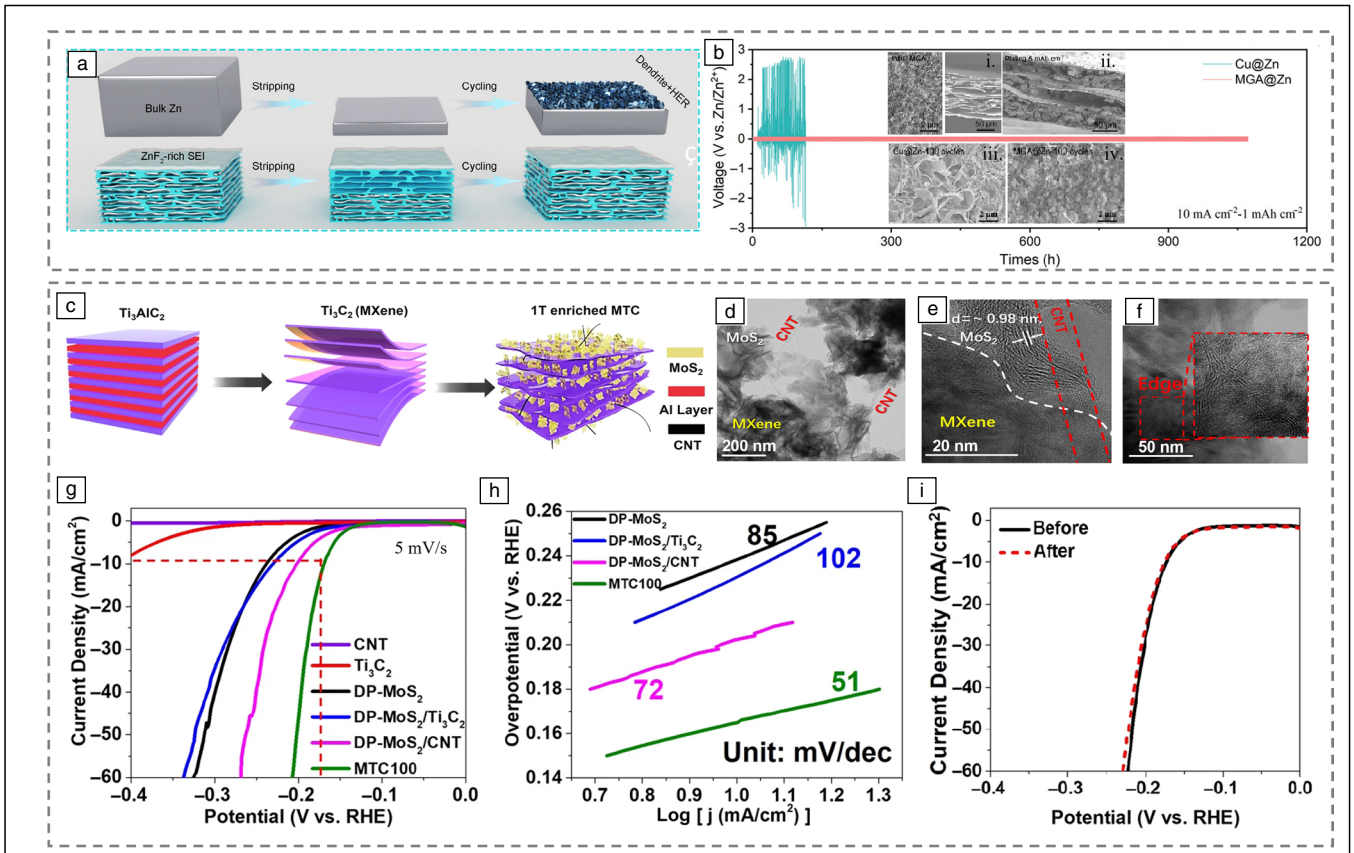

Figure 4. (a) Schematic illustration of Zn plating and cycling on bulk Zn foil and MGA@Zn electrodes. (b) Long-term cycling performance of Cu@Zn and MGA@Zn symmetric cells. The insets are scanning electron microscopy images of initial MGA (i), MGA after plating (ii), Cu@Zn (iii), and MGA@Zn (iv) after 100 cycles. Reprinted with permission from Reference 131. © 2021 Wiley. (c) Schematic illustrations of the preparation process of MoS_2/MXene/carbon nanotube (CNT) (MTC) composite. The transmission electron microscopy image (TEM) (d) and high-resolution TEM images (e, f) of the MTC composite. (g) Polarization curves and (h) Tafel plots for selected samples. (i) The polarization curves of MTC before and after 1000 cycles of CV scans.[146] HER, hydrogen evolution reaction; DP, dual phase; RHE, reversible hydrogen electrode; CV, cyclic voltammetry.

interlayer distance of MoS_2 originating from the glucose-assisted synthesis process, the heterostructure showed efficient intercalation of Li^+ and Mg^{2+} simultaneously. Moreover, undesired side reactions and the growth of dendrites were prohibited due to the excellent chemical and structural stability of graphene, leading to a stable charging/discharging process of 500 cycles.[111]

As for HER, we recently synthesized a 2D/2D MoS_2/Ti_3C_2 MXene nanohybrid using a facile bisolvent solvothermal method (Figure 4c). Due to the NH_4^+ intercalation, MoS_2 layers exhibited expanded interlayer spacing along with partial 2H to 1 T phase transition. The dual-phase MoS_2 (DP-MoS_2) nanosheets with enriched edge sites (Figure 4f) were found in the interlayers as well as the surface of MXene. Sandwiching the DP-MoS_2 with Ti_3C_2 MXene not only prevented the 2D layers from restacking, but also protected the MXene from oxidation.[145] The importance of mixing materials with different dimensionalities was noticed when introducing 1D CNTs into the 2D/2D hybrids. We found that the presence of CNT largely improved the HER performance despite its low density. This can be attributed to the cross-linking function of 1D tubes, which bridged the 2D islands to form a highly conductive network (Figure 4d–e). The MTC configuration outperformed the other binary counterparts in HER with the lowest overpotential of 169 mV and the smallest Tafel slope of 51 mV dec^{-1} (Figure 4g–h). The ternary structure retained a high HER performance after 1000 cycles of CV scans, indicating the promising structural stability of the hybrid (Figure 4i).[146] In addition, the property of the 2D/2D hybrids can be further tailored by introducing prelithiation treatment. We recently employed an n-Buli-based prelithiation process to the hybrid 2D/2D structure and demonstrated that deep phase transition of MoS_2 can be triggered along with the removal of F-containing functional groups in MXene, beneficial for the overall conductivity and ion diffusion kinetics of the composite.[146]

Zero-dimensional/2D MLDHs

Integrating 0D materials with 2D structures can avoid the self-aggregation of 0D QDs and introduce defects on the 2D substrates with favorable properties. The controllable coupling between the two components allows for the design of specific interfaces that promote efficient electron transfer and facilitate energy-storage and catalytic reactions. Various 0D/2D MLDHs

such as carbon QDs/graphene,[147,148] graphene QDs/MoS_2,[149,150] MoS_2 nanoparticles/graphene,[151,152] $Ti_3C_2T_x$ QDs/carbon nanosheets,[153] and $Mo_2C/Ti_3C_2T_x$[154] have been reported.

For instance, the 0D/2D BPQD/TNS composite shown in Figure 2d–f was adopted as the anode material in both LIBs and SIBs. Anchoring the BPQDs on TNS not only enhanced the conductivity of BPQDs, but also relieved the stress generated during cycling. Additionally, the presence of P–O–Ti interfacial bonds between the two components induces atomic charge polarization, resulting in additional pseudocapacitance in TNS. Benefiting from the improved charge adsorption and efficient interfacial electron transfer originated from the mixed dimensionality, high capacity (910 mAh g^{-1} at 100 mA g^{-1}) and long cycling stability (2400 cycles with capacity retention over 100%) were achieved in the LIB system. Moreover, the MLDHs also delivered a high initial capacity of 723 mAh g^{-1} at 50 mA g^{-1} in the SIB system.[96]

Wang et al. anchored Ti_3C_2 MXene quantum dots clusters (QDCs) on N-doped carbon nanosheets for Li-O_2 batteries using the hydrothermal method. The MXene QDC with crystal defects embracing grain boundaries and edge defects were evenly distributed on the 2D carbon nanosheets (**Figure 5**a–b). The defect-rich MXene QDC acted as active centers, contributing to an optimized electronic structure for high catalytic activity. Importantly, the presence of multiscale defects altered the coordination states surrounding the Ti atoms, leading to charge delocalization and *d*-orbit electronic environment optimization at active sites, resulting in enhanced electrocatalytic performance. As the cathode catalyst, the hybrids delivered a high capacity and good cycling stability, as shown in Figure 5c–e.[153]

For HER, Wang et al. built N-doped carbon encapsulated Mo_2C nanodots on $Ti_3C_2T_x$ MXene ($Mo_2C/Ti_3C_2T_x$@NC) using a dopamine-assisted thermal decomposition method (Figure 5f). The N-doped carbon layer was formed from self-polymerized dopamine on the surface of $Ti_3C_2T_x$ and protected the MXene from oxidation during the synthesis. The surface of $Ti_3C_2T_x$ flakes was uniformly decorated with high-density ultrasmall Mo_2C nanodots with an average diameter of 1.1 nm (Figure 5g and h) after the annealing process. The MLDHs demonstrated a comparable overpotential with the Pt/C electrode (Figure 5i) and a Tafel slope of 40 mV dec^{-1} (Figure 5j), which can be attributed to the synergetic effects of hybrid structure in terms of abundant active sites originated from the highly dispersed ultrasmall Mo_2C nanodots and a

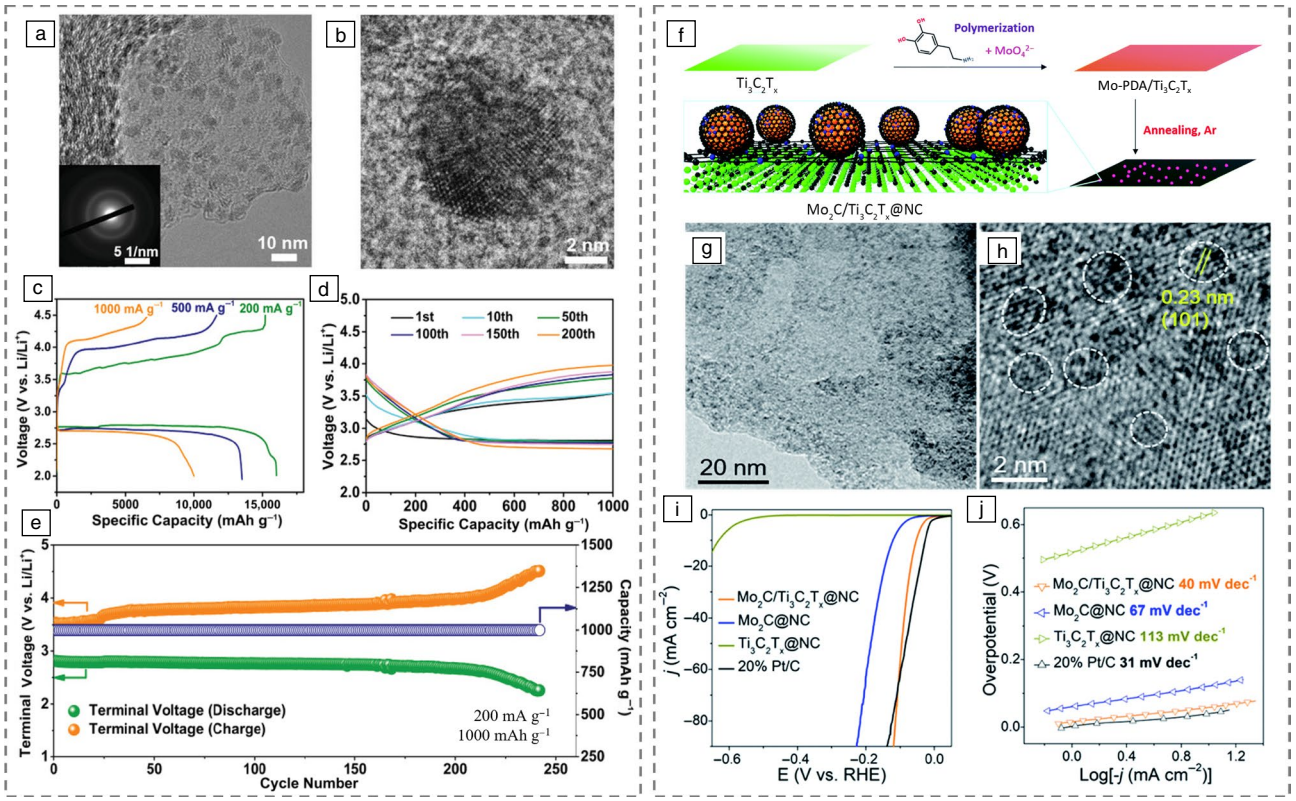

Figure 5. (a, b) High-resolution transmission electron microscopy images of Ti_3C_2 quantum dot clusters/nitrogen-doped carbon nanosheet (QDCs/N-C). The deep discharge–charge curves of the Ti_3C_2 QDC/N-C electrode in Li-O_2 batteries at different current densities (c) and different cycles (d). (e) Cycling stability and terminal discharge–charge voltages of the Ti_3C_2 QDC/N-C electrode. Reprinted with permission from Reference 153. © 2021 Wiley. (f) Schematic illustrations of the $Mo_2C/Ti_3C_2T_x$@NC. (g) TEM image and (h) high-angle annular dark field-scanning TEM image of $Mo_2C/Ti_3C_2T_x$@NC. Polarization curves (i) and Tafel plots (j) for selected samples. Reprinted with permission from Reference 154. © 2020 Royal Society of Chemistry. RHE, reversible hydrogen electrode.

low-resistance electron pathway associated with the coupling of Mo_2C and $Ti_3C_2T_x$ MXene.[154]

One-dimensional/2D MLDHs

A variety of 1D/2D MLDHs, including CNT/MoS_2,[155–158] CNT/$MoSe_2$,[159] CNT/WSe_2,[160] CNT/$Ti_3C_2T_x$,[161–163] CNT/graphene,[164] carbon nanofiber/MoS_2,[165–168] graphene nano cable/MoS_2,[169] and WS_2 nanotube/graphene[170] have been synthesized and investigated for energy storage. For instance, leveraging the structure synergy mentioned previously in Figure 3, the (MoS_2/CF)@MoS_2@C composite demonstrated a high reversible Na^+ storage capacity of 575.3 mAh g^{-1} at 0.1 A g^{-1}.[27] Another example, Li et al. synthesized a core–shell MoS_{2-x}@CNTs composite as a cathode catalyst in Li-O_2 batteries via a hydrothermal method followed by $NaBH_4$ reduction processing (**Figure 6**a). The MoS_2 nanoflakes were found to be uniformly coated on the CNT network (Figure 6b) with randomly distributed sulfur vacancies (Figure 6c–d) induced by the reduction process. The hybrid 1D/2D structure showed high charge/discharge capacities and stable cycle life lasting for 355 cycles at 200 mA g^{-1} with a fixed specific capacity of 500 mAh g^{-1} (Figure 6e). The excellent performance can be ascribed to the synergetic effect of the 1D/2D structure hybridization associated with the suppression of side reactions originating from reduced CNT exposure and enhanced participation of active sites such as S vacancies for the catalytic reaction.[158]

Xu et al. prepared unsaturated S edge-enriched MoS_2 nanosheets on carbon fibers (S-MoS_2@C) via a thermal decomposition method. The uniform distribution of MoS_2 on the carbon layers was confirmed with an ordered, porous 1D/2D structure (Figure 6g–i). Importantly, unsaturated sulfur edges created via ion pre-intercalation treatment (Figure 6f) and the formation of the C–S bonds ensured the existence of plausible active sites and strong interaction between 2D MoS_2 nanosheets and 1D carbon fibers, respectively, resulting in promising HER performance. The hybrid MLDHs exhibit a low overpotential of 136 mV, a Tafel slope of 99 mV dec^{-1}, and a stable catalytic profile over 24 h at a current density of 10 mA cm^{-2} with no obvious morphology change (Figure 6j–l).[168]

Mechanics understanding of electrochemical processes based on vdW-based MLDHs

Two-dimensional vdW heterostructures and MLDHs present unique opportunities for elucidating the governing principles of ion diffusion mechanism and charge-transfer kinetics

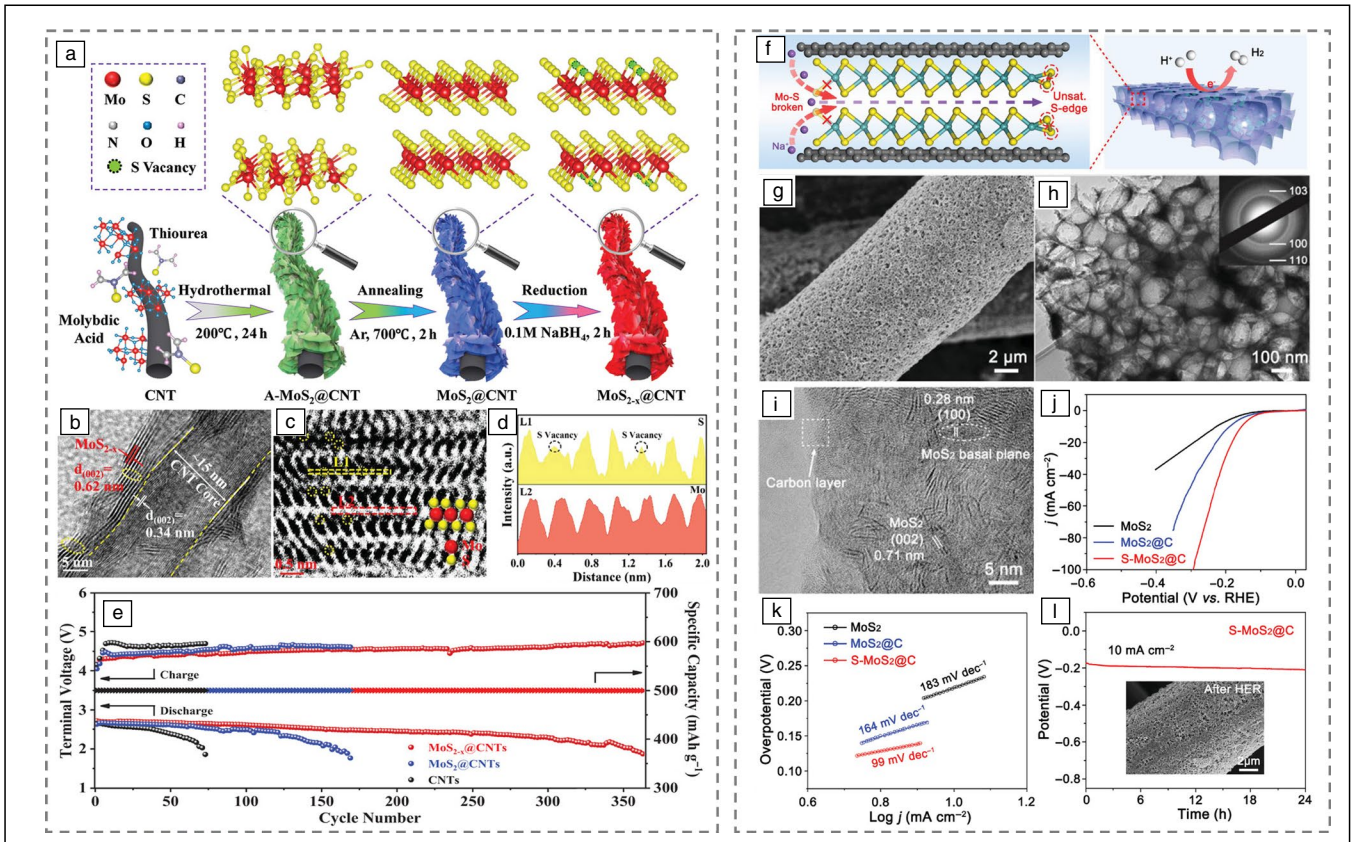

Figure 6. (a) Schematic illustration of the synthesis process for MoS_{2-x}@carbon nanotubes (CNTs). High-resolution transmission electron microscopy (HRTEM) image (b), scanning TEM image (c), and the corresponding intensity profile for MoS_{2-x}@CNTs (d). (e) Cycling performance of different cathodes. Reprinted with permission from Reference 158. © 2021 Wiley. (f) Schematic of the S-MoS_2@C microstructure; (g) SEM, (h) TEM, and (i) HRTEM images of S-MoS_2@C. (j) Polarization curves, (k) Tafel plots, and (l) stability tests for the S-MoS_2@C electrocatalyst. Reprinted with permission from Reference 168. © 2018 Wiley. HER, hydrogen evolution reaction. RHE, reversible hydrogen electrode.

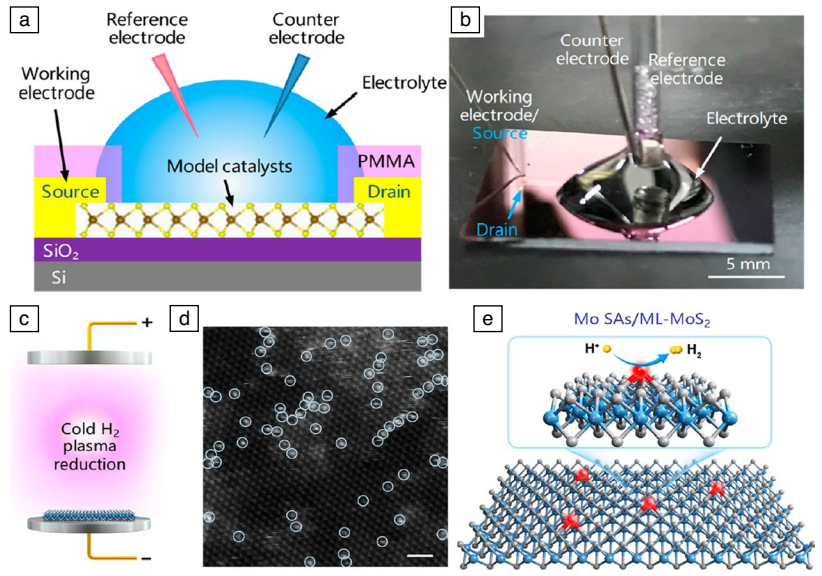

Figure 7. The schematic illustration (a) and optical image (b) show the electrochemical microreactor based on a monolayer (ML)-MoS_2 flake. (c) Schematic showing the synthesis of metal single atoms (SAs) on a cogenetic 2D monolayer by cold hydrogen plasma reduction. (d) Mo SAs/ML-MoS_2 sample, showing high densities of Mo SAs in the sample. (e) Schematic showing Mo SAs/ML-MoS_2 as an active site for hydrogen evolution. Reprinted with permission from Reference 183. © 2020 American Chemical Society.

at electrified interfaces. By leveraging the reduced dimensionality along with novel material assembly/isolation techniques, these materials can be integrated into microreactor platforms.[21,171,172] A typical microreactor device is shown in **Figure 7**a where metal contact is placed on a Si/SiO_2 substrate and acts as a working electrode when put in contact with the material of interest. The exposure area of the active material is well-defined on a micrometer scale with the assistance of e-beam lithography. Electrochemical measurements can be conducted by placing a droplet of electrolyte over the exposed area (Figure 7b).

Combining with ultraflat 2D vdW layers, the microreactor not only enables real-time analysis of electrochemical processes with precise geometrical and environmental control, but also allows one to decouple the impacts of different contributing factors, advancing the fundamental understanding of the energy storage and conversion process at the mechanistic level. For instance, insights on lithium diffusion kinetics and the heterointerface impact on intercalation mechanisms in various 2D vdW layers and their heterostructures were revealed, promoting the rational design of future battery electrodes.[173,174] In addition, impacts of charge injection from the substrate to catalysts, interlayer/intralayer electron transport, stain, and vacancies on HER kinetics were also elucidated based on the microreactor platform.[171,175–182] For instance, Luo et al. synthesized a hybrid 0D/2D structure where isolated Mo single atoms (SAs) were anchored on structurally well-defined 2D monolayer MoS_2 using the cold hydrogen plasma reduction method (Figure 7c–d). A typical two-terminal microreactor with a well-defined exposure area of Mo SAs/MoS_2 was fabricated. Due to the precisely defined catalyst area with a ratio of interfacial surface area to the surface area of electrode close to 1, quantitative analysis of HER kinetics was obtained. In conjunction with DFT calculation, the author concluded that Mo SAs on MoS_2 are efficient sites (Figure 7e) for HER with ultrafast hydrogen adsorption/desorption kinetics, originating from a strong hybridization between the single Mo atoms and hydrogen atoms.[183]

In addition, Yu et al. fabricated a microreactor based on twisted bilayer graphene (**Figure 8**a) and observed a strong twist-angle dependence of heterogeneous charge-transfer kinetics with the greatest electrochemical activity enhancement observed near the "magic angle" (1.1°), as shown in Figure 8b. The activity enhancement was attributed to the MS-derived flat band formation (Figure 8c and d), where strong electron–electron interactions with localized electronic states can be induced,[56,184,185] advancing electron transfer kinetics across the 2D layers. This pioneering work suggests that the twist-angle-derived MS in 2D vdW materials offers an extra degree of freedom for improving the charge-transfer kinetics across 2D vdW layers with the potential to activate the MS as active sites (i.e., topological defects) on 2D basal planes, providing an effective strategy to further advance the performance of a broad range of electrochemical processes based on 2D vdW layers and their MLDHs.[58]

Conclusion and outlook

In this article, we introduced representative techniques for constructing vdW-based heterostructures and MLDHs and discussed their applications in electrochemical energy storage and conversion. Recent advancements in elucidating charge-transport dynamics based on vdW-microreactors were also reviewed. In the end, we will summarize potential strategies to overcome inherent material issues in 2d vdW layers to assist future device performance boosting.

First, to maintain the large reaction area and efficient electron/ion-transport pathways, it is important to prevent 2D vdW layers from restacking and form a universal conductive network in the MLDHs. As we demonstrated previously, introducing 1D interlayer spacers such as CNT to the 2D framework is a promising strategy.[147] However, it is worth noting that uniform distribution of nanotubes in the hybrids is the key to performance improvement. Proper treatment to functionalize the CNT surface will not only debundle the nanotubes, but also improve their interfacial interaction with vdW layers

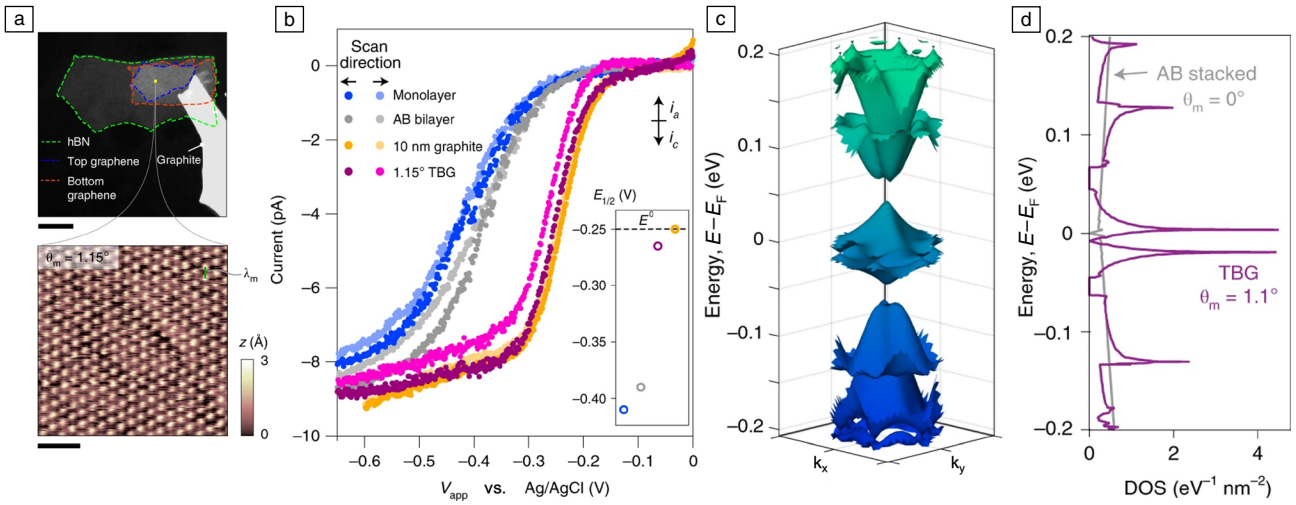

Figure 8. Twisted bilayer graphene (TBG) Moiré superlattices and their electrochemical response. (a) Microscope image (scale bar = 10 μm) of a TBG (twist angle = 1.15°) connected with a graphite contact, and the corresponding scanning transmission microscopy image showing the Moiré patterns. (b) Comparison of steady-state voltammograms using 1.15° bilayer with references using 2 mM $Ru(NH_3)_6^{3+}$ in 0.1 M KCL solution. (c, d) Calculated Moiré band and corresponding density of states (DOS), where E_F is the Fermi energy, k_x and k_y are the reciprocal space vectors. Reprinted with permission from Reference 58. © 2011 Wiley.

without sacrificing the electrical conductivity of the nanotubes. In addition, the contact geometry between the 1D/2D component also determines the overall conductivity of the network. Therefore, attention needs to be paid to engineering the heterostructure contact for structure optimization. Second, it is critical to activate the inert basal planes and increase the total number of active sites in 2D vdW layers and their MLDHs. Recent microreactor-based studies suggested that basal planes can be activated if the charge injection from the substrate to the active material can be improved by reducing the contact resistance between them.[176] Moreover, inducing MS in the twisted bilayer vdW structures can be another important method to improve out-of-plane charge-transfer kinetics as well as forming topological defects to add additional active sites.[58] Nevertheless, the implementation of these fundamental findings into practical electrochemical devices requires extensive experimental efforts on materials synthesis control and cell design optimization. Third, the long-term stability of electrochemical devices using 2D vdW structures has been a longstanding issue. The cause of performance degradation can be a result of material oxidation as well as the intercalant-rich solvent environment. As such, careful study of the dynamics and mechanisms of the degradation process is necessary to evaluate the potential of the vdW-based heterostructure/MLDHs in energy technology and boost their performance in practical applications.

In conclusion, 2D vdW heterostructures and their MLDHs not only provide an excellent material platform for fundamental science exploration, but also present great potential for electrochemical energy applications. Nevertheless, the previously mentioned challenges will need to be well addressed in the future to unlock the complete capabilities of vdW layered structures and their MLDHs for practical industrial adoption. With more time and effort invested in this area, further advancements can be expected and will undoubtedly lead to significant breakthroughs and innovations in the field of electrochemical energy.

Acknowledgments

This work was partially supported by the New York State Center of Excellence in Materials Informatics (CMI) under Award No. C160186, the FuzeHub funding under Award No. 96803, the SUNY SAMRI funding under Award No. 97267, and the National Science Foundation (NSF) under Award No. ECCS-1944095.

Data availability

Not applicable.

Conflict of interest

The authors declare no competing interests.

References

1. Q.H. Wang, K. Kalantar-Zadeh, A. Kis, J.N. Coleman, M.S. Strano, *Nat. Nanotechnol.* **7**, 699 (2012)
2. M. Chhowalla, D. Jena, H. Zhang, *Nat. Rev. Mater.* **1**, 16052 (2016)
3. J. Wang, F. Ma, M. Sun, *RSC Adv.* **7**, 16801 (2017)
4. D. Jariwala, V.K. Sangwan, L.J. Lauhon, T.J. Marks, M.C. Hersam, *ACS Nano* **8**, 1102 (2014)
5. K.S. Novoselov, D. Jiang, F. Schedin, T.J. Booth, V.V. Khotkevich, S.V. Morozov, A.K. Geim, *Proc. Natl. Acad. Sci. U.S.A.* **102**, 10451 (2005)
6. H. Wang, Z. Lu, S. Xu, D. Kong, J.J. Cha, G. Zheng, P.-C. Hsu, K. Yan, D. Bradshaw, F.B. Prinz, Y. Cui, *Proc. Natl. Acad. Sci. U.S.A.* **110**, 19701 (2013)
7. D. Voiry, H. Yamaguchi, J. Li, R. Silva, D.C.B. Alves, T. Fujita, M. Chen, T. Asefa, V.B. Shenoy, G. Eda, M. Chhowalla, *Nat. Mater.* **12**, 850 (2013)
8. C. Tan H. Zhang, *Chem. Soc. Rev.* **44**, 2713 (2015)

9. A.B. Laursen, S. Kegnæs, S. Dahl, I. Chorkendorff, *Energy Environ. Sci.* **5**, 5577 (2012)
10. H.I. Karunadasa, E. Montalvo, Y. Sun, M. Majda, J.R. Long, C.J. Chang, *Science* **335**, 698 (2012)
11. H. Liu, A.T. Neal, Z. Zhu, Z. Luo, X. Xu, D. Tománek, P.D. Ye, *ACS Nano* **8**, 4033 (2014)
12. L.A. Ponomarenko, A.K. Geim, A.A. Zhukov, R. Jalil, S.V. Morozov, K.S. Novoselov, I.V. Grigorieva, E.H. Hill, V.V. Cheianov, V.I. Fal'ko, K. Watanabe, T. Taniguchi, R.V. Gorbachev, *Nat. Phys.* **7**, 958 (2011)
13. B. Anasori, M.R. Lukatskaya, Y. Gogotsi, *Nat. Rev. Mater.* **2**, 16098 (2017)
14. J. Xie, H. Zhang, S. Li, R. Wang, X. Sun, M. Zhou, J. Zhou, X.W. Lou, Y. Xie, *Adv. Mater.* **25**, 5807 (2013)
15. J. Xie, J. Zhang, S. Li, F. Grote, X. Zhang, H. Zhang, R. Wang, Y. Lei, B. Pan, Y. Xie, *J. Am. Chem. Soc.* **135**, 17881 (2013)
16. C. Tsai, K. Chan, F. Abild-Pedersen, J.K. Nørskov, *Phys. Chem. Chem. Phys.* **16**, 13156 (2014)
17. M. Chhowalla, H.S. Shin, G. Eda, L.-J. Li, K.P. Loh, H. Zhang, *Nat. Chem.* **5**, 263 (2013)
18. B. Hinnemann, P.G. Moses, J. Bonde, K.P. Jørgensen, J.H. Nielsen, S. Horch, I. Chorkendorff, J.K. Nørskov, *J. Am. Chem. Soc.* **127**, 5308 (2005)
19. B. Zhao, Z. Wan, Y. Liu, J. Xu, X. Yang, D. Shen, Z. Zhang, C. Guo, Q. Qian, J. Li, R. Wu, Z. Lin, X. Yan, B. Li, Z. Zhang, H. Ma, B. Li, X. Chen, Y. Qiao, I. Shakir, Z. Almutairi, F. Wei, Y. Zhang, X. Pan, Y. Huang, Y. Ping, X. Duan, X. Duan, *Nature* **591**, 385 (2021)
20. J. Wan, S.D. Lacey, J. Dai, W. Bao, M.S. Fuhrer, L. Hu, *Chem. Soc. Rev.* **45**, 6742 (2016)
21. D.J. Hynek, J.V. Pondick, J.J. Cha, *APL Mater.* **7**, 030902 (2019)
22. J. Mei, T. Liao, Z. Sun, *Energy Environ. Mater.* **5**, 115 (2022)
23. J. Mei, T. Liao, G.A. Ayoko, Z. Sun, *ACS Appl. Mater. Interfaces* **11**, 28205 (2019)
24. J. Mei, T. Liao, H. Spratt, G.A. Ayoko, X.S. Zhao, Z. Sun, *Small Methods* **3**, 1900055 (2019)
25. J. Xue, T. Wu, Y. Dai, Y. Xia, *Chem. Rev.* **119**, 5298 (2019)
26. Y.M. Chen, X.Y. Yu, Z. Li, U. Paik, X.W. Lou, *Sci. Adv.* **2**, e1600021 (2016)
27. C. Cui, Z. Wei, J. Xu, Y. Zhang, S. Liu, H. Liu, M. Mao, S. Wang, J. Ma, S. Dou, *Energy Storage Mater.* **15**, 22 (2018)
28. M. Chen, R.C. Haddon, R. Yan, E. Bekyarova, *Mater. Horiz.* **4**, 1054 (2017)
29. Z. Hu, X. Kuai, J. Chen, P. Sun, Q. Zhang, H.-H. Wu, L. Zhang, *ChemSusChem* **13**, 1485 (2020)
30. J. Jeon, Y. Park, S. Choi, J. Lee, S.S. Lim, B.H. Lee, Y.J. Song, J.H. Cho, Y.H. Jang, S. Lee, *ACS Nano* **12**, 338 (2018)
31. C. Xu, S. Song, Z. Liu, L. Chen, L. Wang, D. Fan, N. Kang, X. Ma, H.-M. Cheng, W. Ren, *ACS Nano* **11**, 5906 (2017)
32. S.H. Choi, S.J. Yun, Y.S. Won, C.S. Oh, S.M. Kim, K.K. Kim, Y.H. Lee, *Nat. Commun.* **13**, 1484 (2022)
33. Y. Xu, Z. Lin, X. Huang, Y. Liu, Y. Huang, X. Duan, *ACS Nano* **7**, 4042 (2013)
34. W.K. Tan, H. Muto, G. Kawamura, Z. Lockman, A. Matsuda, *Nanomaterials* **11**, 181 (2021)
35. Q. Liu, Z. Sun, Y. Dou, J.H. Kim, S.X. Dou, *J. Mater. Chem. A* **3**, 11688 (2015)
36. Z. Yuan, X. Xiao, J. Li, Z. Zhao, D. Yu, Q. Li, *Adv. Sci.* **5**, 1700626 (2018)
37. X. Li, J. Wang, *InfoMat* **2**, 3 (2020)
38. J. He, G. Hartmann, M. Lee, G.S. Hwang, Y. Chen, A. Manthiram, *Energy Environ. Sci.* **12**, 344 (2019)
39. P. Wang, C. Jia, Y. Huang, X. Duan, *Matter* **4**, 552 (2021)
40. S. Wang, S. Zhao, X. Guo, G. Wang, *Adv. Energy Mater.* **12**, 2100864 (2022)
41. P.V. Pham, S.C. Bodepudi, K. Shehzad, Y. Liu, Y. Xu, B. Yu, X. Duan, *Chem. Rev.* **122**, 6514 (2022)
42. M. Kumar, Y. Ando, *J. Nanosci. Nanotechnol.* **10**, 3739 (2010)
43. N. Gupta, S.M. Gupta, S.K. Sharma, *Carbon Lett.* **29**, 419 (2019)
44. S.K. Soni, B. Thomas, V.R. Kar, *Mater. Today Commun.* **25**, 101546 (2020)
45. Y. Zhang, L. Zhang, C. Zhou, *Acc. Chem. Res.* **46**, 2329 (2013)
46. B. Deng, Z. Liu, H. Peng, *Adv. Mater.* **31**, e1800996 (2019)
47. L. Lin, B. Deng, J. Sun, H. Peng, Z. Liu, *Chem. Rev.* **118**, 9281 (2018)
48. C. Backes, A. Abdelkader, C. Alonso, A. Andrieux-Ledier, R. Arenal, J. Azpeitia, N. Balakrishnan, L. Banszerus, J. Barjon, R. Bartali, S. Bellani, C. Berger, R. Berger, M. Bernal, C. Bernard, P. Beton, A. Beyer, A. Bianco, P. Bøggild, M. Garcia-Hernandez, *2D Mater.* **7**, 022001 (2020)
49. Y. Zhang, Y. Yao, M.G. Sendeku, L. Yin, X. Zhan, F. Wang, Z. Wang, J. He, *Adv. Mater.* **31**, 1901694 (2019)
50. Q. Wang, Y. Lei, Y. Wang, Y. Liu, C. Song, J. Zeng, Y. Song, X. Duan, D. Wang, Y. Li, *Energy Environ. Sci.* **13**, 1593 (2020)
51. B. Tang, B. Che, M. Xu, Z.P. Ang, J. Di, H.-J. Gao, H. Yang, J. Zhou, Z. Liu, *Small Struct.* **2**, 2000153 (2021)
52. C. Xu, L. Wang, Z. Liu, L. Chen, J. Guo, N. Kang, X.-L. Ma, H.-M. Cheng, W. Ren, *Nat. Mater.* **14**, 1135 (2015)
53. Y. Gogotsi, *Nat. Mater.* **14**, 1079 (2015)
54. Y. Fan, L. Li, Y. Zhang, X. Zhang, D. Geng, W. Hu, *Adv. Funct. Mater.* **32**, 2111357 (2022)
55. Z. Hu, Q. Liu, S.-L. Chou, S.-X. Dou, *Cell Rep. Phys. Sci.* **2**, 100286 (2021)
56. E.Y. Andrei, A.H. MacDonald, *Nat. Mater.* **19**, 1265 (2020)
57. Y. Li, Y. Hua, N. Sun, S. Liu, H. Li, C. Wang, X. Yang, Z. Zhuang, L. Wang, *Nano Res.* **16**, 8712 (2023)
58. Y. Yu, K. Zhang, H. Parks, M. Babar, S. Carr, I.M. Craig, M. Van Winkle, A. Lyssenko, T. Taniguchi, K. Watanabe, V. Viswanathan, D.K. Bediako, *Nat. Chem.* **14**, 267 (2022)
59. E. Kovalska, P.K. Roy, N. Antonatos, V. Mazanek, M. Vesely, B. Wu, Z. Sofer, *NPJ 2D Mater. Appl.* **5**, 68 (2021)
60. Z. Jiang, W. Zhou, A. Hong, M. Guo, X. Luo, C. Yuan, *ACS Energy Lett.* **4**, 2830 (2019)
61. J. Jin, T. Xiao, Y.-F. Zhang, H. Zheng, H. Wang, R. Wang, Y. Gong, B. He, X. Liu, K. Zhou, *Nanoscale* **13**, 19740 (2021)
62. J. Jeon, Y. Yang, H. Choi, J.-H. Park, B.H. Lee, S. Lee, *Nanophotonics* **9**, 1831 (2020)
63. Y. Li, Z. Li, L. Lei, T. Lan, Y. Li, P. Li, X. Lin, R. Liu, Z. Huang, X. Fen, Y. Ma, *FlatChem* **15**, 100091 (2019)
64. Y. Zhu, L. Li, C. Zhang, G. Casillas, Z. Sun, Z. Yan, G. Ruan, Z. Peng, A.-R.O. Raji, C. Kittrell, R.H. Hauge, J.M. Tour, *Nat. Commun.* **3**, 1225 (2012)
65. S. Li, Y. Luo, W. Lv, W. Yu, S. Wu, P. Hou, Q. Yang, Q. Meng, C. Liu, H.-M. Cheng, *Adv. Energy Mater.* **1**, 486 (2011)
66. Y. Xue, Y. Ding, J. Niu, Z. Xia, A. Roy, H. Chen, J. Qu, Z.L. Wang, L. Dai, *Sci. Adv.* **1**, e1400198 (2015)
67. M. Xiao, X. Li, Q. Song, Q. Zhang, M. Lazzarino, G. Cheng, F.P. Ulloa Severino, V. Torre, *Adv. Mater.* **30**, 1806132 (2018)
68. L.P. Yu, X.H. Zhou, L. Lu, L. Xu, F.J. Wang, *ChemSusChem* **14**, 5079 (2021)
69. L. Li, Y. Guo, Y. Sun, L. Yang, L. Qin, S. Guan, J. Wang, X. Qiu, H. Li, Y. Shang, Y. Fang, *Adv. Mater.* **30**, 1706215 (2018)
70. X. Li, J. Zhu, L. Wang, W. Wu, Y. Fang, *Electrochim. Acta* **258**, 291 (2017)
71. V.B. Kumar, Z.E. Porat, A. Gedanken, *Nanomaterials* **12**, 898 (2022)
72. A.T.N. Nguyen, J.H. Shim, *RSC Adv.* **11**, 12520 (2021)
73. Y. Liu, S. Roy, S. Sarkar, J. Xu, Y. Zhao, J. Zhang, *Carbon Energy* **3**, 795 (2021)
74. L. Cui, X. Ren, M. Sun, H. Liu, L. Xia, *Nanomaterials* **11**, 3419 (2021)
75. L. Yan, Y. Yang, C.-Q. Ma, X. Liu, H. Wang, B. Xu, *Carbon* **109**, 598 (2016)
76. S. Kumar, S.K.T. Aziz, O. Girshevitz, G.D. Nessim, *J. Phys. Chem. C* **122**, 2343 (2018)
77. M.J. Deka, D. Chowdhury, *ChemistrySelect* **2**, 1999 (2017)
78. L. Fan, M. Zhu, X. Lee, R. Zhang, K. Wang, J. Wei, M. Zhong, D. Wu, H. Zhu, *Part. Part. Syst. Charact.* **30**, 764 (2013)
79. X. Ding, *J. Mater. Chem. C* **2**, 3717 (2014)
80. W. Tian, A. VahidMohammadi, Z. Wang, L. Ouyang, M. Beidaghi, M.M. Hamedi, *Nat. Commun.* **10**, 2558 (2019)
81. X. Yu, M.S. Prévot, N. Guijarro, K. Sivula, *Nat. Commun.* **6**, 7596 (2015)
82. M. Mojtabavi, A. VahidMohammadi, K. Ganeshan, D. Hejazi, S. Shahbazmohamadi, S. Kar, A.C.T. van Duin, M. Wanunu, *ACS Nano* **15**, 625 (2021)
83. N. Zhang, S. Huang, Z. Yuan, J. Zhu, Z. Zhao, Z. Niu, *Angew. Chem. Int. Ed.* **60**, 2861 (2021)
84. C. Zhao, X. Wang, J. Kong, J.M. Ang, P.S. Lee, Z. Liu, X. Lu, *ACS Appl. Mater. Interfaces* **8**, 2372 (2016)
85. A. Sikdar, P. Dutta, S.K. Deb, A. Majumdar, N. Padma, S. Ghosh, U.N. Maiti, *Electrochim. Acta* **391**, 138959 (2021)
86. X.-Y. Fu, C.-J. Ma, R.-Y. Shu, Y.-Y. Zhang, H.-B. Jiang, *Appl. Phys. Lett.* **122**, 233102 (2023)
87. T. Yun, J.-S. Kim, J. Shim, D.S. Choi, K.E. Lee, S.H. Koo, I. Kim, H.J. Jung, H.-W. Yoo, H.-T. Jung, S.O. Kim, *ACS Appl. Mater. Interfaces* **9**, 1021 (2017)
88. J. Wang, J. Tang, B. Ding, V. Malgras, Z. Chang, X. Hao, Y. Wang, H. Dou, X. Zhang, Y. Yamauchi, *Nat. Commun.* **8**, 15717 (2017)
89. A.E. Allah, J. Wang, Y.V. Kaneti, T. Li, A.A. Farghali, M.H. Khedr, A.K. Nanjundan, B. Ding, H. Dou, X. Zhang, B. Yoshio, Y. Yamauchi, *Nano Energy* **65**, 103991 (2019)
90. Y. Tian, C. Yang, W. Que, X. Liu, X. Yin, L.B. Kong, *J. Power Sources* **359**, 332 (2017)
91. H. Liu, X. Zhang, Y. Zhu, B. Cao, Q. Zhu, P. Zhang, B. Xu, F. Wu, R. Chen, *Nanomicro Lett.* **11**, 65 (2019)
92. Z. Ye, Y. Jiang, L. Li, F. Wu, R. Chen, *Adv. Mater.* **33**, 2101204 (2021)
93. Y. Dong, H. Shi, Z.-S. Wu, *Adv. Funct. Mater.* **30**, 2000706 (2020)
94. H. Lim, H. Kim, S.-O. Kim, W. Choi, *J. Chem. Eng.* **387**, 124144 (2020)
95. P. Qiu, T. Zhao, Y. Fang, G. Zhu, X. Zhu, J. Yang, X. Li, W. Jiang, L. Wang, W. Luo, *Adv. Funct. Mater.* **31**, 2007496 (2021)
96. R. Meng, J. Huang, Y. Feng, L. Zu, C. Peng, L. Zheng, L. Zheng, Z. Chen, G. Liu, B. Chen, Y. Mi, J. Yang, *Adv. Energy Mater.* **8**, 1801514 (2018)
97. D.T. Pham, T.H. Lee, D.H. Luong, F. Yao, A. Ghosh, V.T. Le, T.H. Kim, B. Li, J. Chang, Y.H. Lee, *ACS Nano* **9**, 2018 (2015)
98. R.K. Singh, R. Kumar, D.P. Singh, R. Savu, S.A. Moshkalev, *Mater. Today Chem.* **12**, 282 (2019)
99. S. Sinha, H. Kim, A.W. Robertson, *Mater. Today Adv.* **12**, 100169 (2021)
100. J. Ren, R.-P. Ren, Y.-K. Lv, *J. Chem. Eng.* **353**, 419 (2018)
101. A. Machín, K. Fontánez, J.C. Arango, D. Ortiz, J. De León, S. Pinilla, V. Nicolosi, F.I. Petrescu, C. Morant, F. Márquez, *Materials* (Basel) **14**, 2609 (2021)
102. F.R. Fan, R. Wang, H. Zhang, W. Wu, *Chem. Soc. Rev.* **50**, 10983 (2021)
103. L. Tang, X. Meng, D. Deng, X. Bao, *Adv. Mater.* **31**, 1901996 (2019)
104. K.R.G. Lim, A.D. Handoko, S.K. Nemani, B. Wyatt, H.-Y. Jiang, J. Tang, B. Anasori, Z.W. Seh, *ACS Nano* **14**, 10834 (2020)

105. Q. Lu, Y. Yu, Q. Ma, B. Chen, H. Zhang, *Adv. Mater.* **28**, 1917 (2016)
106. X. Wang, Q. Weng, Y. Yang, Y. Bando, D. Golberg, *Chem. Soc. Rev.* **45**, 4042 (2016)
107. Y. Fang, Y. Lv, F. Gong, A.A. Elzatahry, G. Zheng, D. Zhao, *Adv. Mater.* **28**, 9385 (2016)
108. D. Sun, D. Ye, P. Liu, Y. Tang, J. Guo, L. Wang, H. Wang, *Adv. Energy Mater.* **8**, 1702383 (2018)
109. T.-T. Shan, S. Xin, Y. You, H.-P. Cong, S.-H. Yu, A. Manthiram, *Angew. Chem. Int. Ed.* **55**, 12783 (2016)
110. R. Wang, S. Wang, D. Jin, Y. Zhang, Y. Cai, J. Ma, L. Zhang, *Energy Storage Mater.* **9**, 195 (2017)
111. X. Fan, R.R. Gaddam, N.A. Kumar, X.S. Zhao, *Adv. Energy Mater.* **7**, 1700317 (2017)
112. Y. Liu, X. Wang, X. Song, Y. Dong, L. Yang, L. Wang, D. Jia, Z. Zhao, J. Qiu, *Carbon* **109**, 461 (2016)
113. Y. Liu, L. Jiao, Q. Wu, Y. Zhao, K. Cao, H. Liu, Y. Wang, H. Yuan, *Nanoscale* **5**, 9562 (2013)
114. X. Han, X. Tong, X. Liu, A. Chen, X. Wen, N. Yang, X.-Y. Guo, *ACS Catal.* **8**, 1828 (2018)
115. Z. Yang, J. Zhu, X. Xu, L. Wang, G. Zhou, Z. Yang, Y. Zhang, *RSC Adv.* **13**, 4056 (2023)
116. Y.-J. Tang, Y. Wang, X.-L. Wang, S.-L. Li, W. Huang, L.-Z. Dong, C.-H. Liu, Y.-F. Li, Y.-Q. Lan, *Adv. Energy Mater.* **6**, 1600116 (2016)
117. Y. Hou, B. Zhang, Z. Wen, S. Cui, X. Guo, Z. He, J. Chen, *J. Mater. Chem. A* **2**, 13795- (2014)
118. M.A. Worsley, S.J. Shin, M.D. Merrill, J. Lenhardt, A.J. Nelson, L.Y. Woo, A.E. Gash, T.F. Baumann, C.A. Orme, *ACS Nano* **9**, 4698 (2015)
119. X. Meng, L. Yu, C. Ma, B. Nan, R. Si, Y. Tu, J. Deng, D. Deng, X. Bao, *Nano Energy* **61**, 611 (2019)
120. Z. Luo, J. Zhou, L. Wang, G. Fang, A. Pan, S. Liang, *J. Mater. Chem. A* **4**, 15302 (2016)
121. H. Tang, K. Dou, C.-C. Kaun, Q. Kuang, S. Yang, *J. Mater. Chem. A* **2**, 360 (2014)
122. S. Deng, Y. Zhong, Y. Zeng, Y. Wang, Z. Yao, F. Yang, S. Lin, X. Wang, X. Lu, X. Xia, J. Tu, *Adv. Mater.* **29**, 1700748 (2017)
123. S. Mao, Z. Wen, S. Ci, X. Guo, K. Ostrikov, J. Chen, *Small* **11**, 414 (2015)
124. Z. Liu, N. Li, H. Zhao, Y. Du, *J. Mater. Chem. A* **3**, 19706 (2015)
125. S.-K. Park, G.D. Park, D. Ko, Y.C. Kang, Y. Piao, *J. Chem. Eng.* **315**, 355 (2017)
126. D. Xiao, C. Huang, Y. Luo, K. Tang, Q. Ruan, G. Wang, P.K. Chu, *ACS Appl. Mater. Interfaces* **12**, 2460 (2020)
127. H. Zhou, F. Yu, J. Sun, R. He, Y. Wang, C.F. Guo, F. Wang, Y. Lan, Z. Ren, S. Chen, *J. Mater. Chem. A* **4**, 9472 (2016)
128. J. Zhang, Q. Wang, L. Wang, X.A. Li, W. Huang, *Nanoscale* **7**, 10391 (2015)
129. Z. Ma, X. Zhou, W. Deng, D. Lei, Z. Liu, *ACS Appl. Mater. Interfaces* **10**, 3634 (2018)
130. W. Bao, X. Xie, J. Xu, X. Guo, J. Song, W. Wu, D. Su, G. Wang, *Chem. Eur. J.* **23**, 12613 (2017)
131. J. Zhou, M. Xie, F. Wu, Y. Mei, Y. Hao, L. Li, R. Chen, *Adv. Mater.* **34**, 2106897 (2022)
132. S. Zhou, X. Yang, W. Pei, N. Liu, J. Zhao, *Nanoscale* **10**, 10876 (2018)
133. S. Hussain, D. Vikraman, Z. Ali Sheikh, M. Taqi Mehran, F. Shahzad, K. Mujasam Batoo, H.-S. Kim, D.-K. Kim, M. Ali, J. Jung, *J. Chem. Eng.* **452**, 139523 (2023)
134. H. Huang, J. Cui, G. Liu, R. Bi, L. Zhang, *ACS Nano* **13**, 3448 (2019)
135. K.R.G. Lim, A.D. Handoko, L.R. Johnson, X. Meng, M. Lin, G.S. Subramanian, B. Anasori, Y. Gogotsi, A. Vojvodic, Z.W. Seh, *ACS Nano* **14**, 16140 (2020)
136. M. Li, Y. Wang, T. Li, J. Li, L. Huang, Q. Liu, J. Gu, D. Zhang, *J. Mater. Chem. A* **9**, 922 (2021)
137. Z. Bojarska, M. Mazurkiewicz-Pawlicka, B. Mierzwa, T. Płociński, Ł. Makowski, *J. Environ. Chem. Eng.* **10**, 108038 (2022)
138. J. Liu, Y. Liu, D. Xu, Y. Zhu, W. Peng, Y. Li, F. Zhang, X. Fan, *Appl. Catal. B Environ.* **241**, 89 (2019)
139. D. Liu, Z. Lv, J. Dang, W. Ma, K. Jian, M. Wang, D. Huang, W. Tian, *Inorg. Chem.* **60**, 9932 (2021)
140. L. Huang, L. Ai, M. Wang, J. Jiang, S. Wang, *Int. J. Hydrog. Energy* **44**, 965 (2019)
141. J. Liang, C. Ding, J. Liu, T. Chen, W. Peng, Y. Li, F. Zhang, X. Fan, *Nanoscale* **11**, 10992 (2019)
142. N. Li, Y. Zhang, M. Jia, X. Lv, X. Li, R. Li, X. Ding, Y.-Z. Zheng, X. Tao, *Electrochim. Acta* **326**, 134976 (2019)
143. S. Hussain, I. Rabani, D. Vikraman, T. Mehran, F. Shahzad, Y.-S. Seo, H.-S. Kim, J. Jung, *Int. J. Energy Res.* **45**, 18770 (2021)
144. K. Yuan, P. Hao, Y. Zhou, X. Hu, J. Zhang, S. Zhong, *Phys. Chem. Chem. Phys.* **24**, 13713 (2022)
145. S. Wei, Y. Fu, P. Roy, X. Tong, H. Yue, M. Liu, H.N. Jaiswal, S. Shahi, Y.I. Gata, T. Butler, H. Li, Q. Jia, F. Yao, *ACS Appl. Mater. Interfaces* **14**, 35673 (2022)
146. S. Wei, Y. Fu, M. Liu, H. Yue, S. Park, Y.H. Lee, H. Li, F. Yao, *NPJ 2D Mater. Appl.* **6**, 25 (2022)
147. Z. Liu, L. Zhang, L. Sheng, Q. Zhou, T. Wei, J. Feng, Z. Fan, *Adv. Energy Mater.* **8**, 1802042 (2018)
148. Y. Jin, C. Hu, Q. Dai, Y. Xiao, Y. Lin, J.W. Connell, F. Chen, L. Dai, *Adv. Funct. Mater.* **28**, 1804630 (2018)
149. Riyanto, I. Sahroni, K. Bindumadhavan, P.-Y. Chang, R.-A. Doong, *Front. Chem.* **7**, 116 (2019)
150. B. Guo, K. Yu, H. Li, R. Qi, Y. Zhang, H. Song, Z. Tang, Z. Zhu, M. Chen, *ACS Appl. Mater. Interfaces* **9**, 3653 (2017)
151. Y. Li, H. Wang, L. Xie, Y. Liang, G. Hong, H. Dai, *J. Am. Chem. Soc.* **133**, 7296 (2011)
152. H. Dong, C. Liu, H. Ye, L. Hu, B. Fugetsu, W. Dai, Y. Cao, X. Qi, H. Lu, X. Zhang, *Sci. Rep.* **5**, 17542 (2015)
153. P. Wang, D. Zhao, X. Hui, Z. Qian, P. Zhang, Y. Ren, Y. Lin, Z. Zhang, L. Yin, *Adv. Energy Mater.* **11**, 2003069 (2021)
154. H. Wang, Y. Lin, S. Liu, J. Li, L. Bu, J. Chen, X. Xiao, J.-H. Choi, L. Gao, J.-M. Lee, *J. Mater. Chem. A* **8**, 7109 (2020)
155. S. Chong, L. Sun, C. Shu, S. Guo, Y. Liu, W. Wang, H.K. Liu, *Nano Energy* **63**, 103868 (2019)
156. X. Zhang, F. Zhou, S. Zhang, Y. Liang, R. Wang, *Adv. Sci.* **6**, 1900090 (2019)
157. F. Yang, P. Hu, F.F. Yang, B. Chen, F. Yin, K. Hao, R. Sun, L. Gao, Z. Sun, K. Wang, Z. Yin, *Small* (2023). https://doi.org/10.1002/smll.202301468
158. D. Li, L. Zhao, Q. Xia, J. Wang, X. Liu, H. Xu, S. Chou, *Adv. Funct. Mater.* **32**, 2108153 (2022)
159. Y. Huang, H. Lu, H. Gu, J. Fu, S. Mo, C. Wei, Y.-E. Miao, T. Liu, *Nanoscale* **7**, 18595 (2015)
160. X. Wang, Y. Chen, F. Qi, B. Zheng, J. He, Q. Li, P. Li, W. Zhang, Y. Li, *Electrochem. Commun.* **72**, 74 (2016)
161. M. Estili, S. Matsuda, L. Jia, N. Sakai, R. Ma, T.S. Suzuki, K. Uosaki, *Nanoscale* **15**, 8289 (2023)
162. X. Wang, S. Wang, J. Qin, X. Xie, R. Yang, M. Cao, *Inorg. Chem.* **58**, 16524 (2019)
163. P. Zhang, R. Wang, T. Xiao, Z. Chang, Z. Fang, Z. Zhu, C. Xu, L. Wang, J. Cheng, *Energy Technol.* **8**, 2000306 (2020)
164. Y. Shi, W. Gao, H. Lu, Y. Huang, L. Zuo, W. Fan, T. Liu, *ACS Sustain. Chem. Eng.* **5**, 6994 (2017)
165. C. Zhao, C. Yu, M. Zhang, Q. Sun, S. Li, M. Norouzi Banis, X. Han, Q. Dong, J. Yang, G. Wang, X. Sun, J. Qiu, *Nano Energy* **41**, 66 (2017)
166. H. Zhu, F. Lyu, M. Du, M. Zhang, Q. Wang, J. Yao, B. Guo, *ACS Appl. Mater. Interfaces* **6**, 22126 (2014)
167. C. Zhao, J. Kong, X. Yao, X. Tang, Y. Dong, S.L. Phua, X. Lu, *ACS Appl. Mater. Interfaces* **6**, 6392 (2014)
168. Q. Xu, Y. Liu, H. Jiang, Y. Hu, H. Liu, C. Li, *Adv. Energy Mater.* **9**, 1802553 (2019)
169. D. Kong, H. He, Q. Song, B. Wang, W. Lv, Q.-H. Yang, L. Zhi, *Energy Environ. Sci.* **7**, 3320 (2014)
170. R. Chen, T. Zhao, W. Wu, F. Wu, L. Li, J. Qian, R. Xu, H. Wu, H.M. Albishri, A.S. Al-Bogami, D.A. El-Hady, J. Lu, K. Amine, *Nano Lett.* **14**, 5899 (2014)
171. Y. Zhou, J.L. Silva, J.M. Woods, J.V. Pondick, Q. Feng, Z. Liang, W. Liu, L. Lin, B. Deng, B. Brena, F. Xia, H. Peng, Z. Liu, H. Wang, C.M. Araujo, J.J. Cha, *Adv. Mater.* **30**, 1706076 (2018)
172. S. Yazdani, M. Yarali, J.J. Cha, *Nano Res.* **12**, 2126 (2019)
173. D.K. Bediako, M. Rezaee, H. Yoo, D.T. Larson, S.Y.F. Zhao, T. Taniguchi, K. Watanabe, T.L. Brower-Thomas, E. Kaxiras, P. Kim, *Nature* **558**, 425 (2018)
174. M. Kühne, F. Paolucci, J. Popovic, P.M. Ostrovsky, J. Maier, J.H. Smet, *Nat. Nanotechnol.* **12**, 895 (2017)
175. D. Voiry, R. Fullon, J. Yang, C. de Carvalho Castro e Silva, R. Kappera, I. Bozkurt, D. Kaplan, M.J. Lagos, P.E. Batson, G. Gupta, A.D. Mohite, L. Dong, D. Er, V.B. Shenoy, T. Asefa, M. Chhowalla, *Nat. Mater.* **15**, 1003 (2016)
176. Y. Zhou, J.V. Pondick, J.L. Silva, J.M. Woods, D.J. Hynek, G. Matthews, X. Shen, Q. Feng, W. Liu, Z. Lu, Z. Liang, B. Brena, Z. Cai, M. Wu, L. Jiao, S. Hu, H. Wang, C.M. Araujo, J.J. Cha, *Small* **15**, 1900078 (2019)
177. G. Li, Z. Chen, Y. Li, D. Zhang, W. Yang, Y. Liu, L. Cao, *ACS Nano* **14**, 1707 (2020)
178. D.R. Cummins, U. Martinez, A. Sherehiy, R. Kappera, A. Martinez-Garcia, R.K. Schulze, J. Jasinski, J. Zhang, R.K. Gupta, J. Lou, M. Chhowalla, G. Sumanasekera, A.D. Mohite, M.K. Sunkara, G. Gupta, *Nat. Commun.* **7**, 11857 (2016)
179. Y. Yu, G.-H. Nam, Q. He, X.-J. Wu, K. Zhang, Z. Yang, J. Chen, Q. Ma, M. Zhao, Z. Liu, F.-R. Ran, X. Wang, H. Li, X. Huang, B. Li, Q. Xiong, Q. Zhang, Z. Liu, L. Gu, Y. Du, W. Huang, H. Zhang, *Nat. Chem.* **10**, 638 (2018)
180. X. Liu, B. Li, X. Li, A.R. Harutyunyan, J. Hone, D.V. Esposito, *Nano Lett.* **19**, 8118 (2019)
181. J. Wang, M. Yan, K. Zhao, X. Liao, P. Wang, X. Pan, W. Yang, L. Mai, *Adv. Mater.* **29**, 1604464 (2017)
182. W. Zhang, X. Liao, X. Pan, M. Yan, Y. Li, X. Tian, Y. Zhao, L. Xu, L. Mai, *Small* **15**, 1900964 (2019)
183. Y. Luo, S. Zhang, H. Pan, S. Xiao, Z. Guo, L. Tang, U. Khan, B.-F. Ding, M. Li, Z. Cai, Y. Zhao, W. Lv, Q. Feng, X. Zou, J. Lin, H.-M. Cheng, B. Liu, *ACS Nano* **14**, 767 (2020)

184. Y. Cao, V. Fatemi, S. Fang, K. Watanabe, T. Taniguchi, E. Kaxiras, P. Jarillo-Herrero, *Nature* **556**, 43 (2018)
185. K. Seo, V.N. Kotov, B. Uchoa, *Phys. Rev. Lett.* **122**, 246402 (2019) □

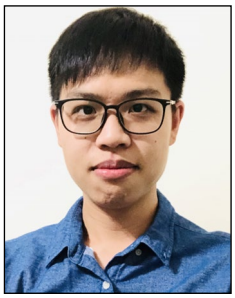

Chu Te Chen is a doctoral candidate in the Department of Materials Design and Innovation at the University at Buffalo, The State University of New York. He received his MSc degree in earth and environmental sciences from National Chung Cheng University, Taiwan, in 2019. His research focuses on the synthesis of nanomaterials and the fabrication of energy-storage and electronic applications. Chen can be reached by email at chuteche@buffalo.edu.

Yu Fu is a doctoral candidate in the Department of Materials Design and Innovation at the University at Buffalo, The State University of New York, where he also received his master's degree in 2021. His research focuses on the synthesis of nanomaterials for energy-storage and conversion applications. Fu can be reached by email at yfu5@buffalo.edu.

Xin Gao is an assistant research fellow at Harbin University of Science and Technology, China. He received his PhD degree in materials science from Harbin University of Science and Technology in 2019. His research interests include the synthesis, characterization, and applications of two-dimensional nanomaterials. Gao can be reached by email at gaoxin6825@126.com.

Anthony Butler is an undergraduate student in the Department of Materials Design and Innovation at the University at Buffalo, The State University of New York. He will be graduating in 2024 and plans to attend graduate school in the same department. His research focuses on chemical vapor deposition of two-dimensional materials for semiconductor applications and batteries. Butler can be reached by email at afbutler@buffalo.edu.

Kristofer Reyes is an assistant professor in the Department of Materials Design and Innovation at the University at Buffalo, The State University of New York. He received his PhD degree in applied and interdisciplinary mathematics from the University of Michigan in 2013. His research interests include applied mathematics for computational chemistry and materials science; machine-learning algorithms applied to materials science, and kinetic Monte Carlo methods in materials simulation. Reyes can be reached by email at kreyes3@buffalo.edu.

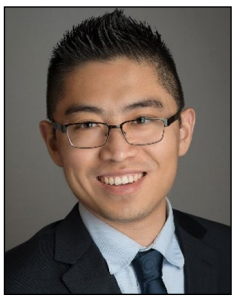

Huamin Li received his PhD degree from Sungkyunkwan University, Korea, and completed postdoctoral research from the University of Notre Dame. His expertise is in the exploration of two-dimensional materials and their application for high-performance energy-efficient nanoelectronics. He is currently serving as an associate editor member for *IEEE Access*, *Nano Express*, and *Materials Research Letters*; a technical committee member (nanoelectronics) for the IEEE Nanotechnology Council, and an executive council member for the 2D Materials Technical Group at the American Vacuum Society. Li can be reached by email at huaminli@buffalo.edu.

Michael Pentaris joined Custom Electronics, Inc. in 2003 as vice president and was promoted to president and CEO in 2004. In 2005, he started a new product development program and in 2007, custom-created loxus, an ultra capacitor manufacturer. Pentaris was a dual CEO for both Custom Electronics and loxus until late 2010. He received his bachelor's and master's degrees from Binghamton University, The State University of New York. Pentaris can be reached by email at mpentaris@customelec.com.

Ajay Yadav joined Applied Materials, Inc. in 2018 and works as a process engineer on the Advanced Product and Technology Development Team. He received his BS degree in materials and metallurgical engineering from the Indian Institute of Technology, Kanpur (India). He received his PhD degree in materials science and engineering from the University of California, Berkeley, for work on novel phenomena in oxide superlattices.Yadav conducted postdoctoral research in the Department of Electrical Engineering and Computer Sciences at the University of California, Berkeley, on negative capacitance in oxide ferroelectrics. He has experience in process technologies related to deposition, etch, and anneals. Yadav can be reached by email at ajay_yadav@amat.com.

Keith T. Wong is a process engineering manager on the Advanced Product and Technology Development Team at Applied Materials, Inc. He earned his BS degree in chemical engineering from Cornell University before completing his PhD degree in chemical engineering at Stanford University researching fundamental surface chemistry on semiconductor surfaces by *in situ* spectroscopic and computational methods. He was a postdoctoral researcher at the California Institute of Technology. He has experience in developing deposition, surface modification, and etch processes for advanced technology nodes. Wong can be reached by email at keith_wong@amat.com.

Hongyan Yue has been a professor at Harbin University of Science and Technology, China, since 2013. He received his PhD degree in materials physics and chemistry from Harbin Institute of Technology, China, in 2009. He was a visiting researcher at Sungkyunkwan University, China, from 2011 to 2013, and then at Case Western Reserve University in 2016. His current research interests focus on two-dimensional nanomaterials, including graphene and metal dichalcogenides, and their applications in biosensors, energy storage, etc. Yue can be reached by email at hyyue@hrbust.edu.cn.

Fei Yao is an assistant professor in the Department of Materials Design and Innovation at the University at Buffalo, The State University of New York. She received her dual PhD degrees in energy science from Sungkyunkwan University, Korea, and in physics from École Polytechnique, France, in 2013. She worked as a postdoctoral researcher in the Center for Integrated Nanostructure Physics, Korea, and in the Department of Electrical Engineering at the University of Notre Dame. Her research interests include low-dimensional materials synthesis and applications in energy storage and conversion. Yao can be reached by email at feiyao@buffalo.edu.